Electronic Supplementary Material (ESI) for Analyst.

Supporting Information

Aqueous dependent sensing of hydrazine and phosphate anions using bis-heteroleptic Ru(II) Complex with phthalimide anchored pyridine-triazole ligand

Mohanraj Ramachandran[a], Asad Syed,[b] Najat Marraiki,[b] and Sambandam Anandan*[a]

[a]Department of Chemistry, National Institute of Technology, Tiruchirappalli 620 015, India

[b]Department of Botany & Microbiology, College of Science, King Saud University, Riyadh 11451, Saudi Arabia

TABLE OF CONTENT

No.	Content	Fig. No.
1.	^{1}H NMR spectrum of TpN_3 in $CDCl_3$	**Fig. S1**
2.	^{13}C NMR spectrum of TpN_3 in $CDCl_3$	**Fig. S2**
3.	^{1}H NMR spectrum of TpH in $CDCl_3$	**Fig. S3**
4.	^{13}C NMR spectrum of TpH in $CDCl_3$	**Fig. S4**
5.	^{1}H NMR spectrum of TpI in $CDCl_3$	**Fig. S5**
6.	^{13}C NMR spectrum of TpI in $CDCl_3$	**Fig. S6**
7.	^{1}H NMR spectrum of RtpH in CD_3CN	**Fig. S7**
8.	^{1}H NMR spectrum of RtpH in DMSO-d_6	**Fig. S8**
9.	Expanded ^{1}H NMR spectrum of RtpH in DMSO-d_6	**Fig. S9**
10.	^{13}C NMR spectrum of RtpH in DMSO-d_6	**Fig. S10**
11.	^{1}H NMR spectrum of RtpI in DMSO-d_6	**Fig. S11**
12.	^{13}C NMR spectrum of RtpI in DMSO-d_6	**Fig. S12**
13.	HR ESI- Mass spectrum of TpH	**Fig. S13**
14.	HR ESI- Mass spectrum of RtpH	**Fig. S14**
15.	HR ESI- Mass spectrum of tpI	**Fig. S15**
16.	HR ESI- Mass spectrum of RtpI	**Fig. S16**
17.	FT-IR spectra for compound TpN_3,TpH, TpI, RtpH and RtpI	**Fig. S17**
18.	(A) UV-Vis spectra of RtpH (10 μM) with various anions (5 equiv.) phosphate anions and ($H_2PO_4^-$ and $H_2P_2O_7^{2-}$) (1 equiv.), (B) Uv-Vis spectra of RtpI (25 μM) with various anions (10 equiv.) and phosphate anions ($H_2PO_4^-$ and $H_2P_2O_7^{2-}$) (1 equiv.) in CH_3CN.	**Fig. S18**
19.	(A) UV-Vis spectra of RtpH (10 μM) with the addition of $H_2PO_4^-$ anions (0-1 equiv.), (B) Uv-Vis spectra of RtpH (10 μM) with the addition of $H_2PO_4^-$ anions (0-1 equiv.) in CH_3CN.	**Fig. S19**
20.	(A) UV-Vis spectra of RtpI (10 μM) with the addition of $H_2PO_4^-$ anions (0-1 equiv.), (B) Uv-Vis spectra of RtpI (10 μM) with the addition of $H_2PO_4^-$ anions (0-1 equiv.) in CH_3CN.	**Fig. S20**
21.	(A) Under UV light illumination, RtpH with different anions (B) Under UV light illumination, RtpI with various types of anions	**Fig. S21**
22.	(A) Emission intensity of RtpH (10 μM) with different metal ions (10 equiv.), (B) Emission intensity of RtpI	**Fig. S22**

	(10 μM) with different metal ions (10 equiv.) in CH_3CN.	
23.	Time course study of RtpH (10 μM) upon addition different equivalent of $H_2PO_4^-$ (A) $H_2P_2O_7^{2-}$ (B) in CH_3CN and Time course study of RtpI (10 μM) upon addition different equivalent of $H_2PO_4^-$ (C) $H_2P_2O_7^{2-}$ (D) in CH_3CN.	**Fig.S23**
24.	Job's plot of RtpH with (A) $H_2PO_4^-$ (B) $H_2P_2O_7^{2-}$, Job's plot of RtpI with (C) $H_2PO_4^-$ (D) $H_2P_2O_7^{2-}$	**Fig. S24**
25.	Benesi-Hildebrand plot from emission titration data of RtpH (10 μM) with $H_2PO_4^-$ (A) and $H_2P_2O_7^{2-}$ (B) and of RtpI with $H_2PO_4^-$ (C) and $H_2P_2O_7^{2-}$ (D).	**Fig. S25**
26.	(A) Interference study of RtpH (10 μM) with and without $H_2PO_4^-$ anions in presence of different anions (10 equiv.), (B) Interference study of RtpI (10 μM) with and without $H_2PO_4^-$ anions in presence of different anions (10 equiv.)	**Fig. S26**
27.	Linear plot of RtpH with (A) $H_2PO_4^-$ (B) $H_2P_2O_7^2$, Linear plot of RtpI with (C) $H_2PO_4^-$ (D) $H_2P_2O_7^2$	**Fig. S27**
28.	The emission intensity of metalloreceptors (RtpH and RtpI, 10 μM) with phosphate anions ($H_2PO_4^-$ and $H_2P_2O_7^{2-}$, 10 μM) upon varying water percentage with CH_3CN	**Fig. S28**
29.	(A) ^1H NMR titration of RtpH with $H_2PO_4^-$ in CD_3CN/D_2O (9/1, v/v), (B) ^1H NMR titration of RtpI with $H_2PO_4^-$ in CD_3CN/D_2O (9/1, v/v)	**Fig. S29**
30.	(A) Cyclic Voltammetry (A and B) and Differential Pulse Voltammetry (C and D) of metalloreceptors (RtpH and RtpI) with and without phosphate and anions.	**Fig. S30**
31.	(A) UV-Vis spectra of RtpH (25 μM) with various anions (10 equiv.) and hydrazine (4 equiv.), (B) Uv-Vis spectra of RtpI (25 μM) with various anions (10 equiv.) and hydrazine (4 equiv.) in CH_3CN/H_2O (6/4, v/v).	**Fig. S31**
32.	(A) UV-Vis spectra of RtpH (25 μM) with the gradual addition of hydrazine (4 equiv.), (B) Uv-Vis spectra of RtpI (25 μM) with the gradual addition of hydrazine (4 equiv.) in CH_3CN/H_2O (6/4, v/v).	**Fig. S32**
33.	The emission intensity of metalloreceptors (RtpH and RtpI, 25 μM) with hydrazine (100 μM) upon varying water percentage with CH_3CN	**Fig. S33**
34.	Time course study of RtpH (25 μM) upon addition different equivalent of hydrazine (B) Time course study of RtpH (25 μM) upon addition different equivalent of hydrazine	**Fig. S34**
35.	(A) Job's plot of RtpH with hydrazine , (B) Job's plot of RtpI with hydrazine	**Fig. S35**
36.	(A) Linear plot of RtpH with hydrazine , (B) Linear plot of RtpI with hydrazine	**Fig. S36**
37.	(A) Non linear fitting of RtpH (25 μM) upon addition different concentration of Hydrzine (B) Non linear fitting of RtpI (25 μM) upon addition different concentration of Hydrzine	**Fig. S37**

38.	(A) Lifetime decay of RtpH (10 μM) with and without hydrazine (4 equiv.), (B) Lifetime decay of RtpI (10 μM) with and without hydrazine (4 equiv.) in CH_3CN	**Fig. S38**
39.	Partial ^1H NMR spectrum of RtpH-NH_2 in DMSO-d_6	**Fig. S39**
40.	HR-ESI Mass spectra of RtpH-NH_2	**Fig. S40**
41.	HR-ESI Mass spectra of RtpI-NH_2	**Fig. S41**
42.	Cell viability of HeLa cells in the presence of various concentrations of (A) RtpH and (B) RtpI	**Fig. S42**
43.	Cellular uptake (HeLa) image of 25μM RtpH and RtpI	**Fig. S43**
44.	Optimized structure of RtpH, RtpH-NH_2, RtpH-$H_2PO_4^-$ (from left to right)	**Fig. S44**
45.	Optimized structure of RtpI, RtpI-NH_2, RtpI-$H_2PO_4^-$ (from left to right)	**Fig. S45**
46.	Probable reaction mechanism of metalloreceptors (RtpH and RtpI) with hydrazine and phosphate anions	**Fig. S46**
47.	IC_{50} Values for cis-Platin and metalloreceptors against HeLa cells	**Table. S1**

Instruments

The NMR spectra were carried out in Bruker Avance 500 spectrometers using $CDCl_3$, CD_3CN, and DMSO-d_6 solvent (TMS as internal standard) in ppm. The FT-IR spectra were recorded on a Thermo Scientific Nicolet iS5 FT IR Spectrometer. The CHN elemental analysis was carried out from the Vario EL III microanalyzer. UV-Vis and Fluorescence spectra were carried out on Specord S 600 diode-array UV-Vis spectrophotometer and Shimadzu RF-5301 PC spectrofluorophotometer, respectively in RT. The luminescence lifetime was studied with the Time-Correlated Single Photon Counting method (TC-SPC) in a Horiba FluoroMax-4 instrument. The CV and DPV experiment were recorded on an Autolab three-electrode system, where Ag/AgCl as a reference electrode, glassy carbon as a working electrode, and platinum wire as a counter electrode in an acetonitrile solvent containing 0.1 M tetrabutylammonium hexafluorophosphate ($^tBu_4N^+PF_6^-$) as the supporting electrolyte with 100 mV scan rate and the system was calibrated using ferrocene/ferrocenium ion (Fc/Fc^+) standard.

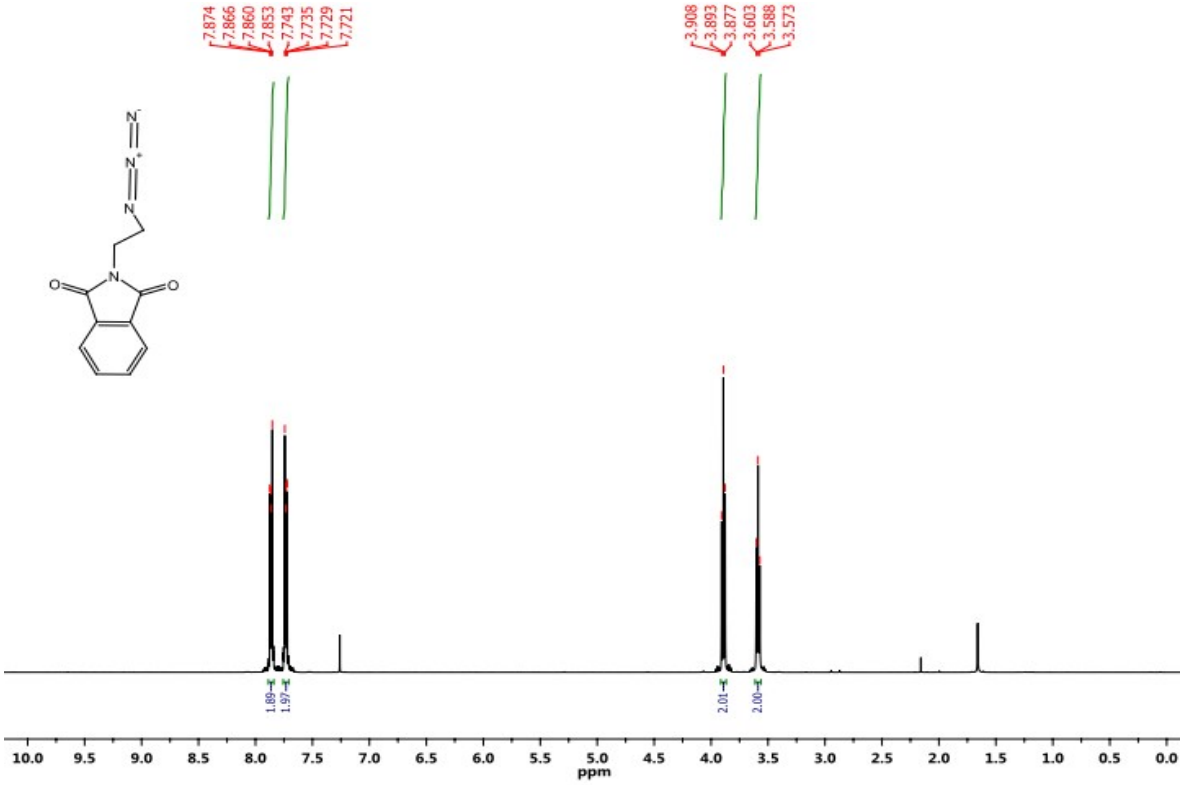

Fig.S1 ^{1}H NMR spectrum of TpN_3 in $CDCl_3$

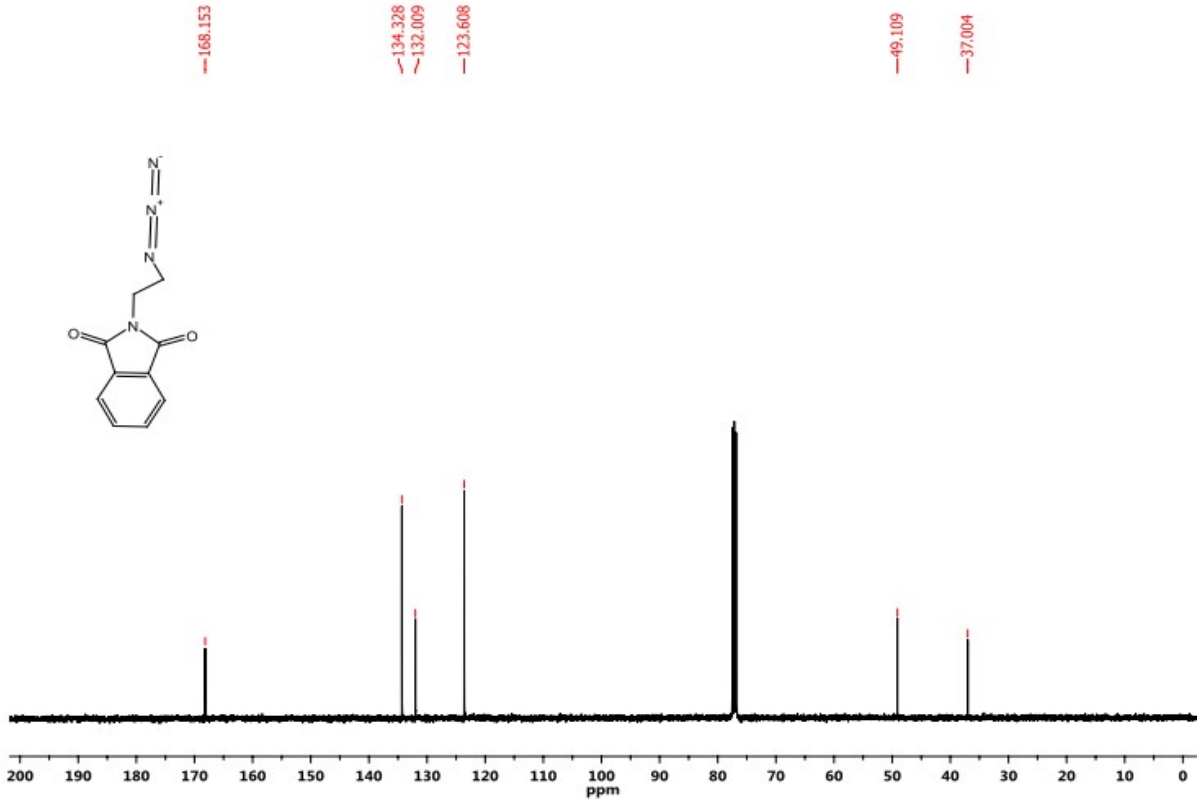

Fig.S2 ^{13}C NMR spectrum of TpN_3 in $CDCl_3$

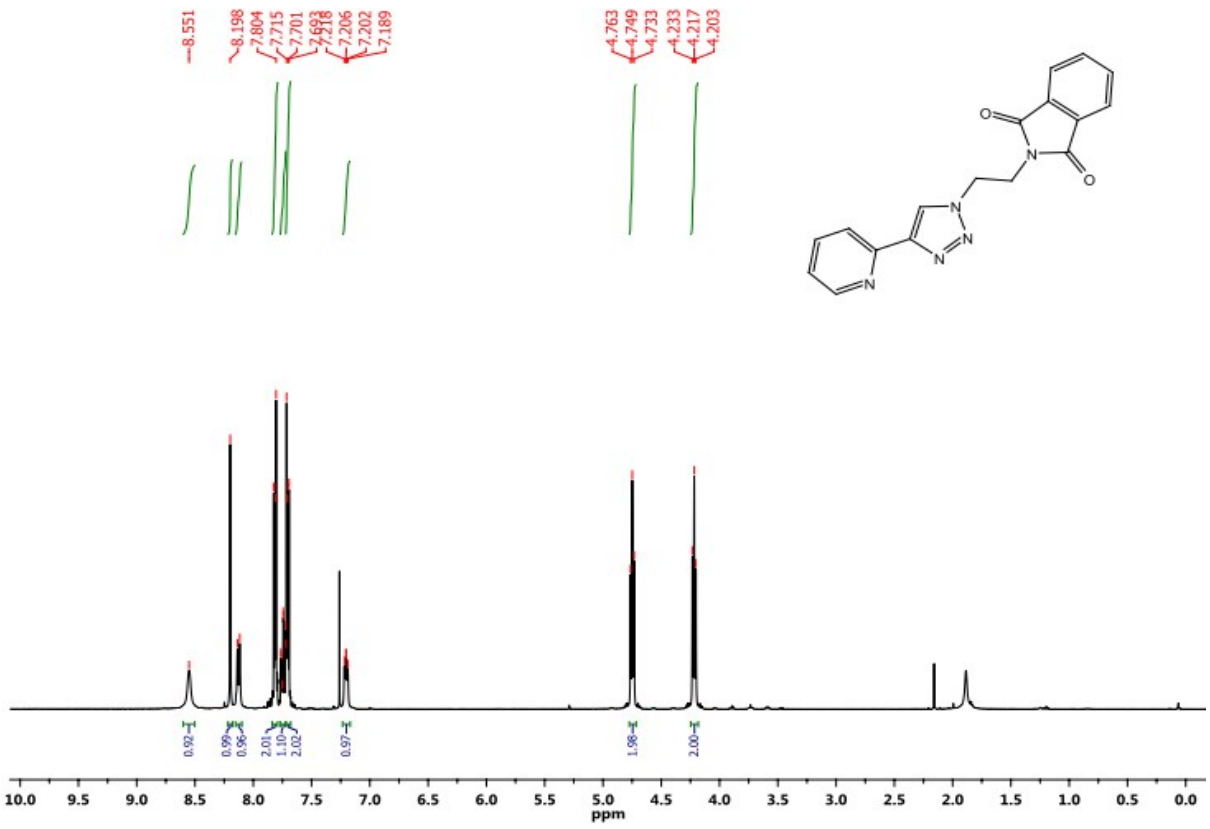

Fig.S3 ^{1}H NMR spectrum of TpH in $CDCl_3$

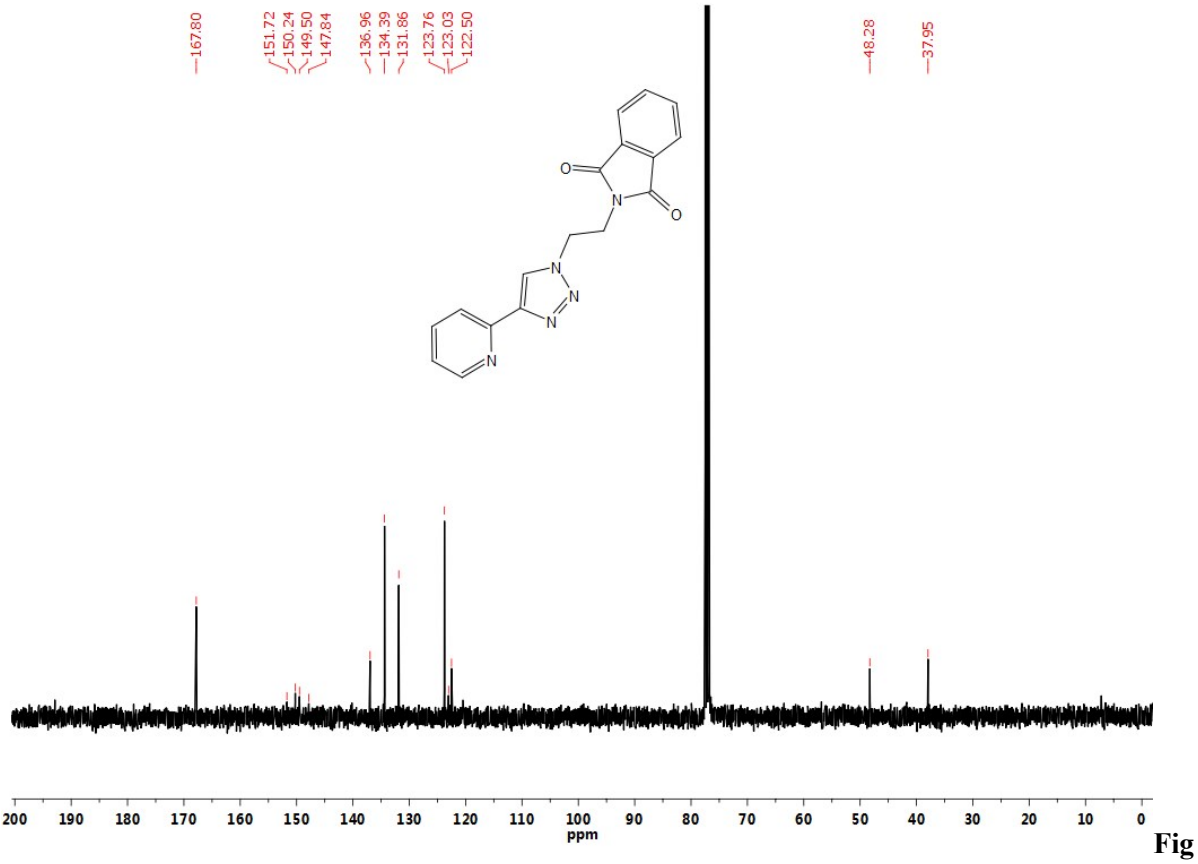

Fig.S4 ^{13}C NMR spectrum of TpH in $CDCl_3$

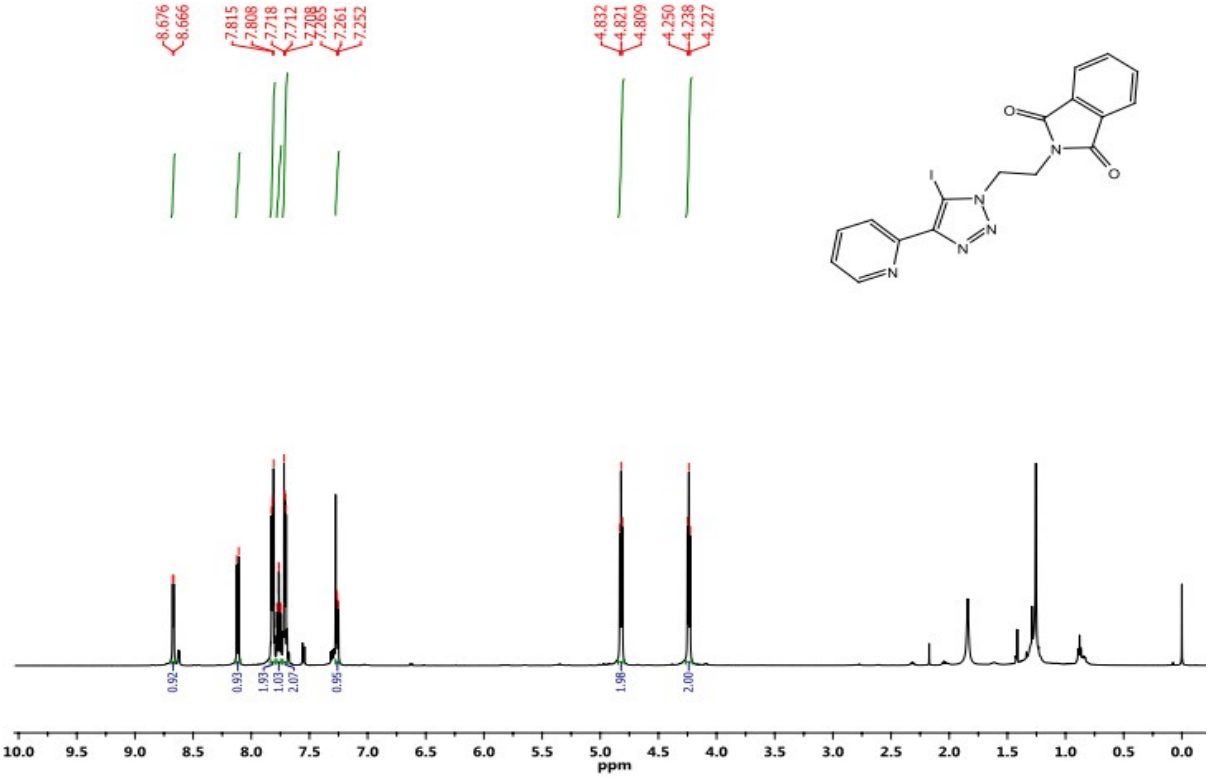

Fig.S5 ^{1}H NMR spectrum of TpI in $CDCl_3$

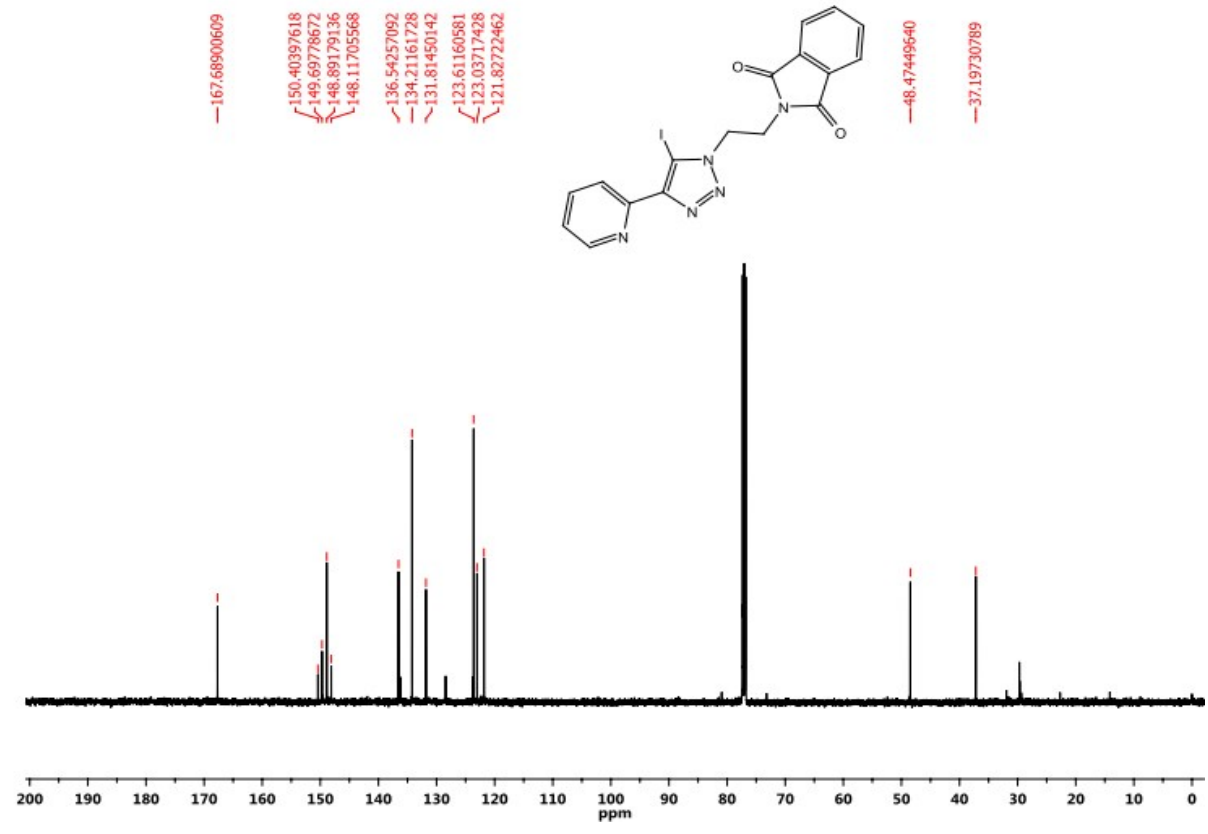

Fig.S6 ^{13}C NMR spectrum of TpI in $CDCl_3$

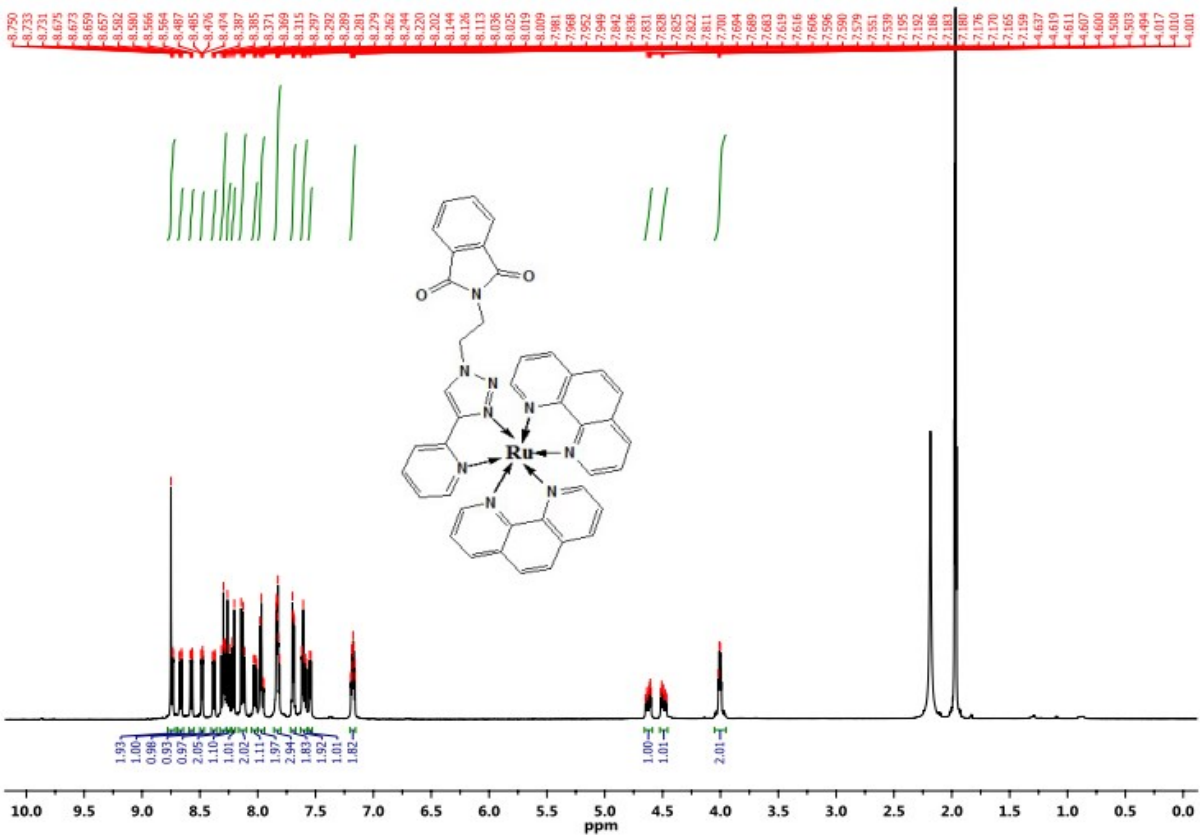

Fig.S7 ^{1}H NMR spectrum of RtpH in CD_3CN

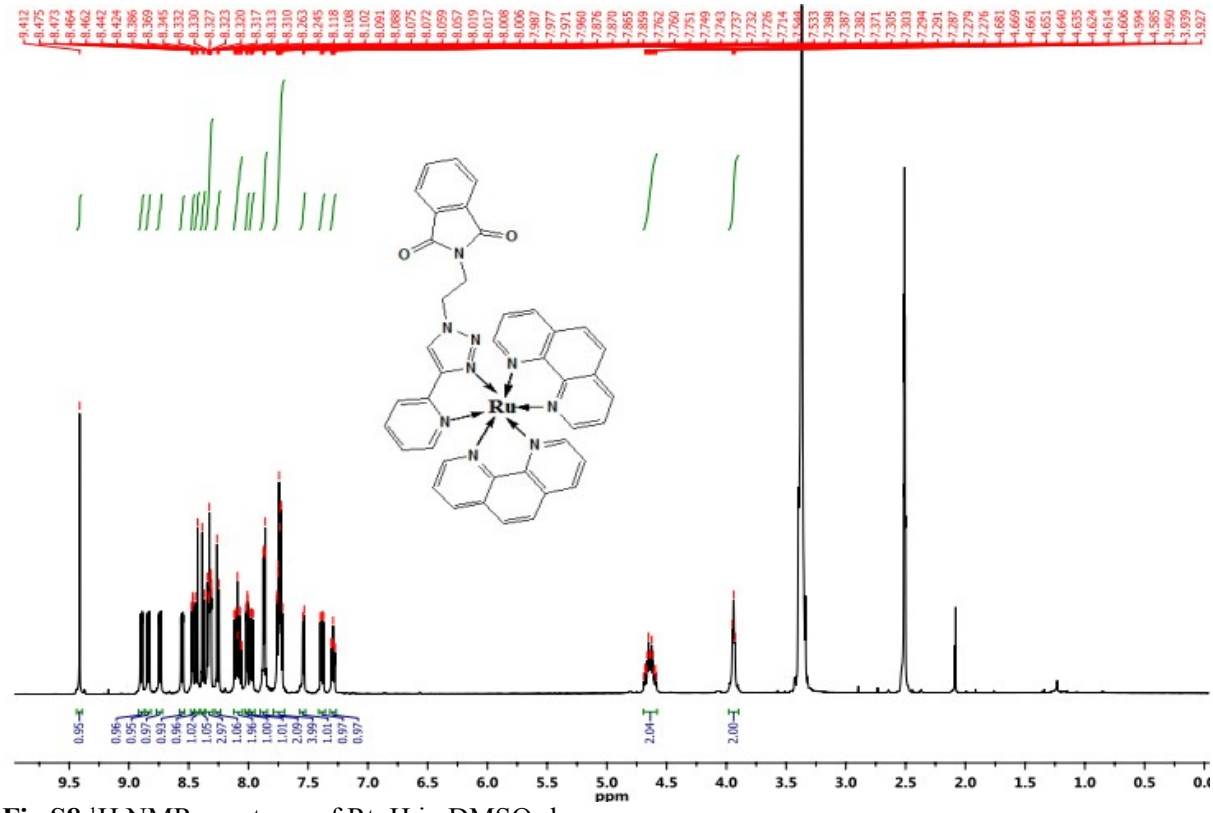

Fig.S8 ^{1}H NMR spectrum of RtpH in DMSO-d_6

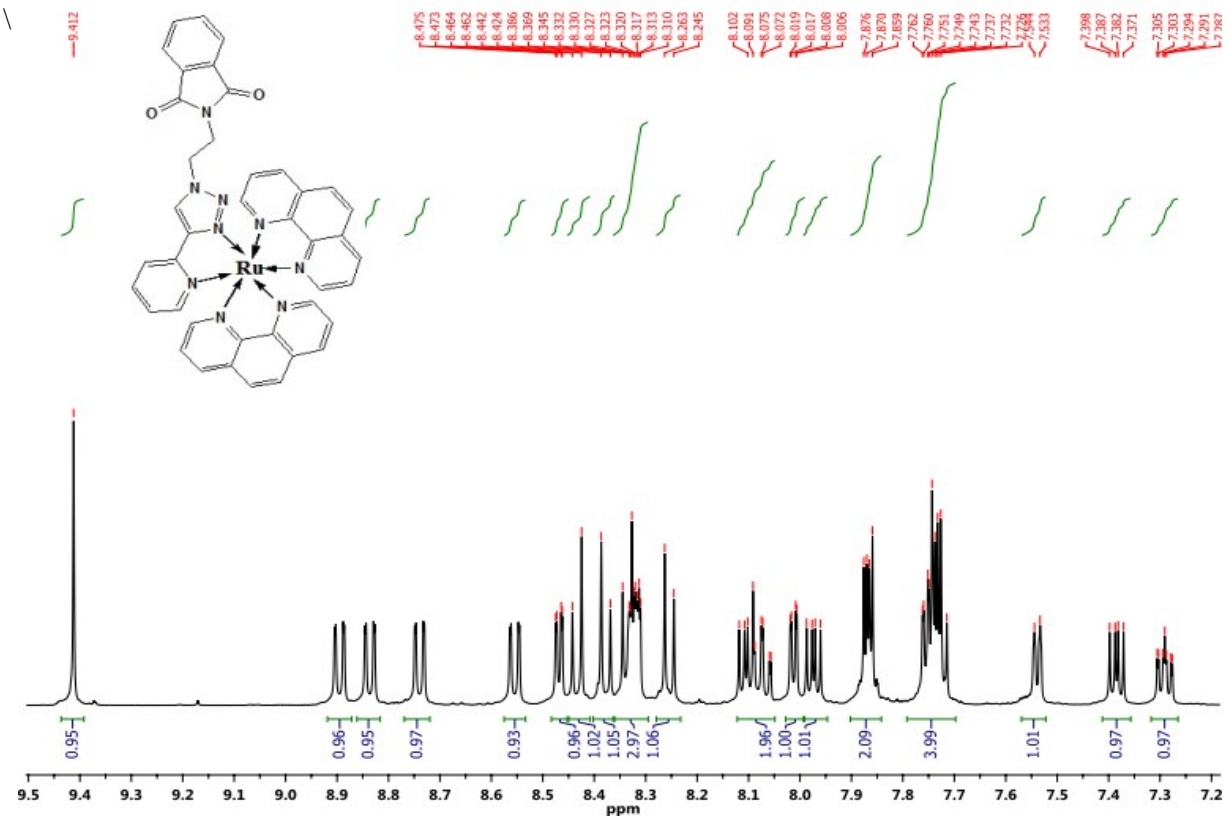

Fig.S9 Expanded ^{1}H NMR spectrum of RtpH in DMSO-d_6

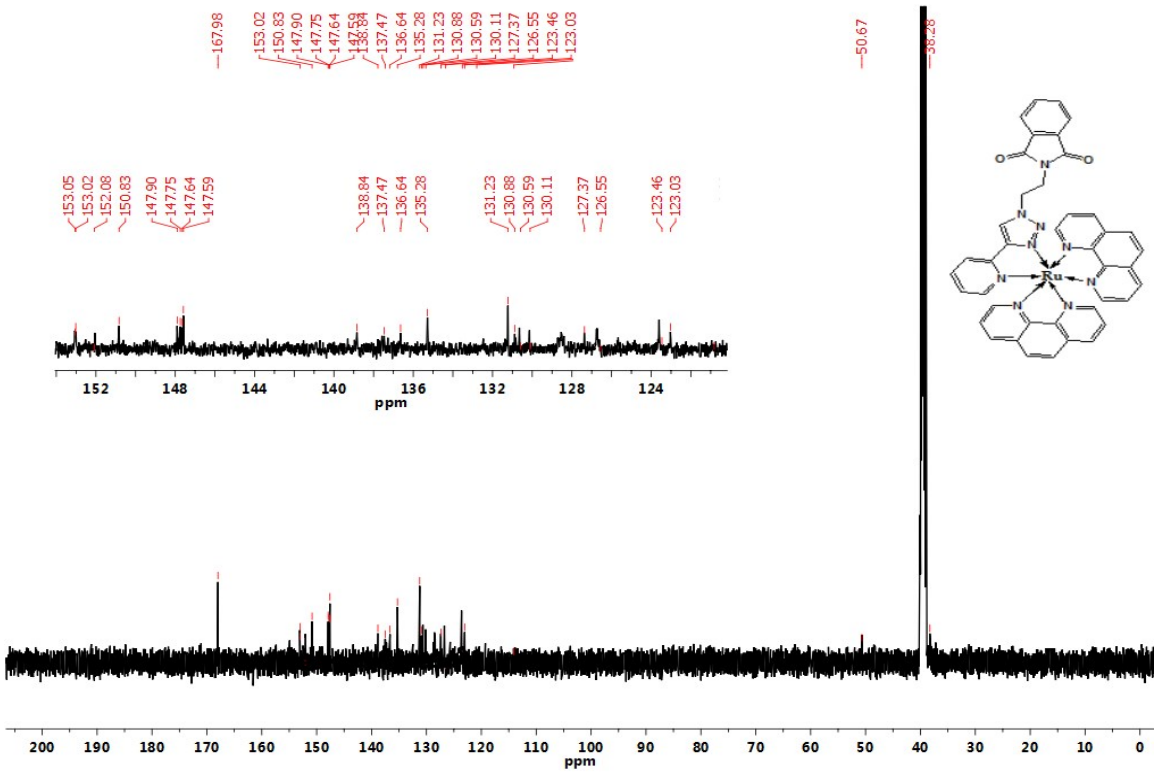

Fig.S10 ^{13}C NMR spectrum of RtpH in DMSO-d_6

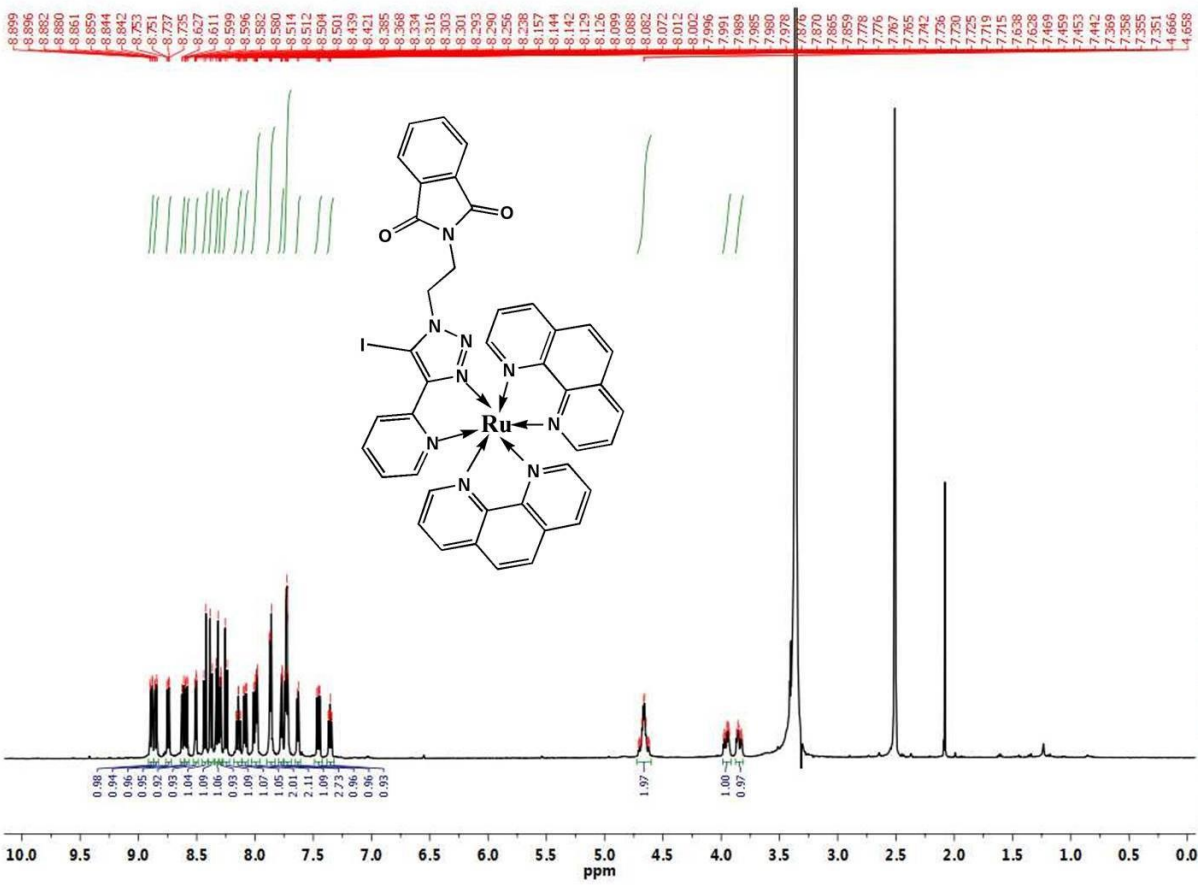

Fig.S11 ^{1}H NMR spectrum of RtpI in DMSO-d_6

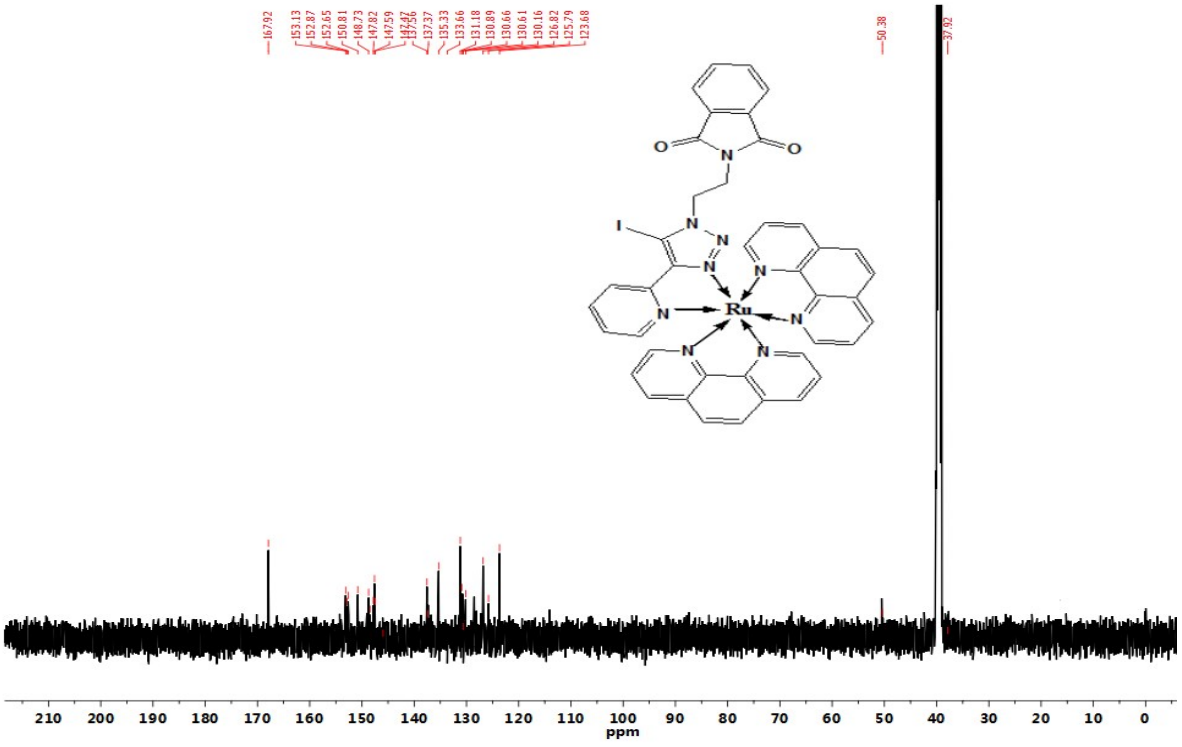

Fig.S12 ^{13}C NMR spectrum of RtpI in DMSO-d_6

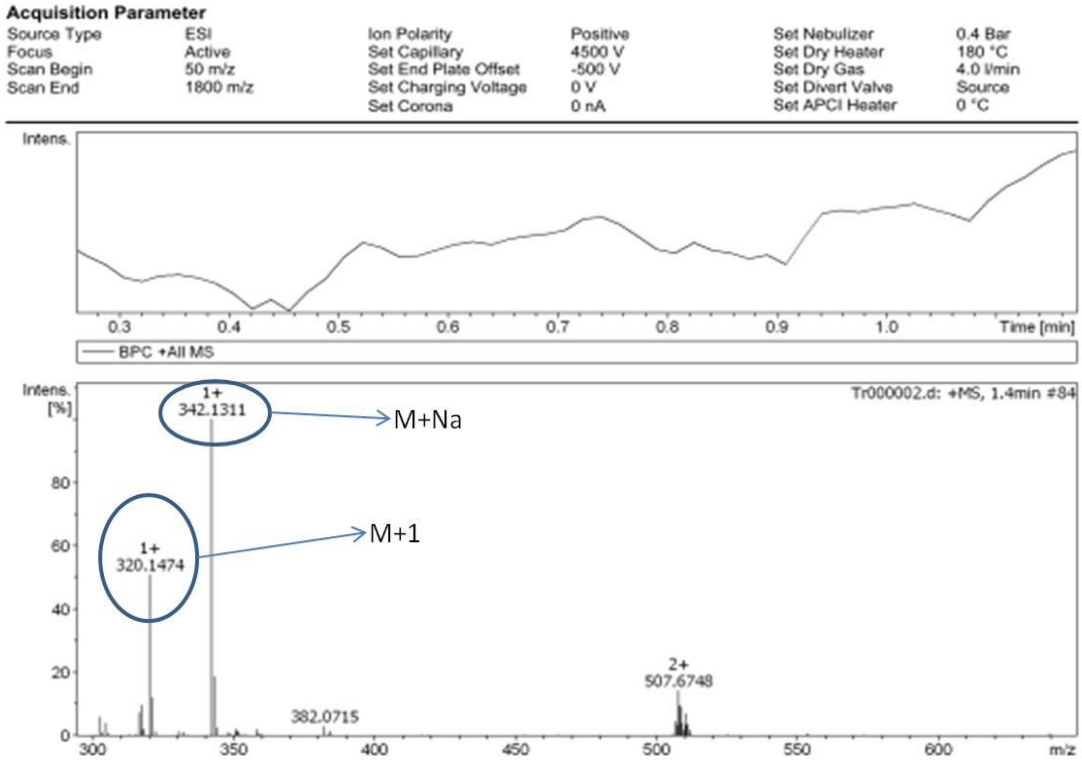

Fig.S13 HR ESI-Mass spectrum of TpH

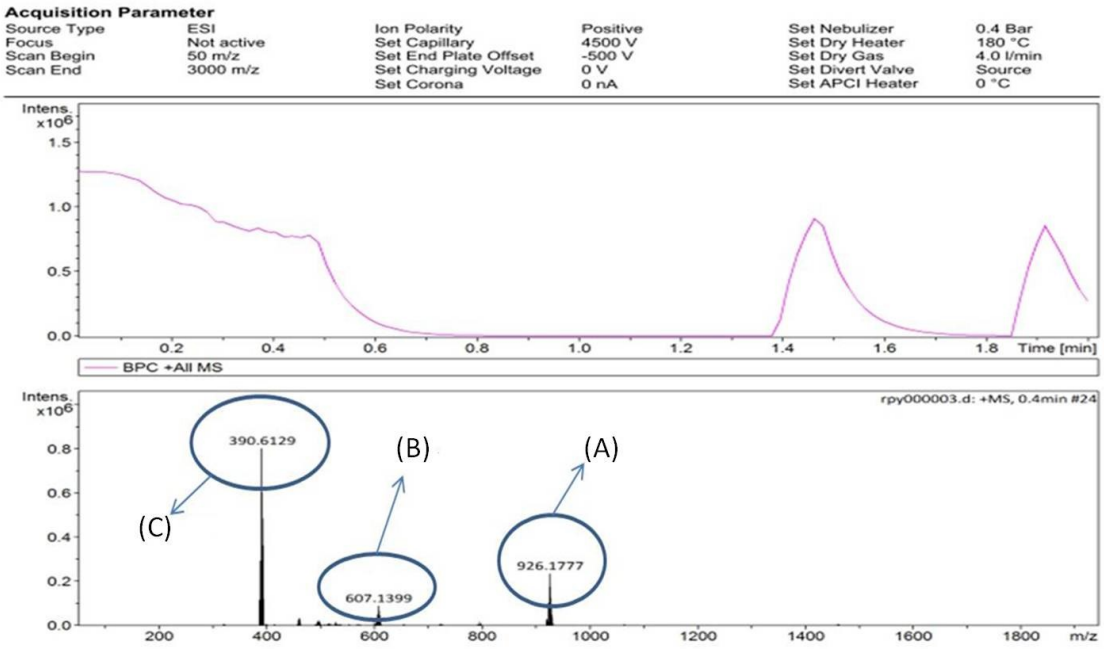

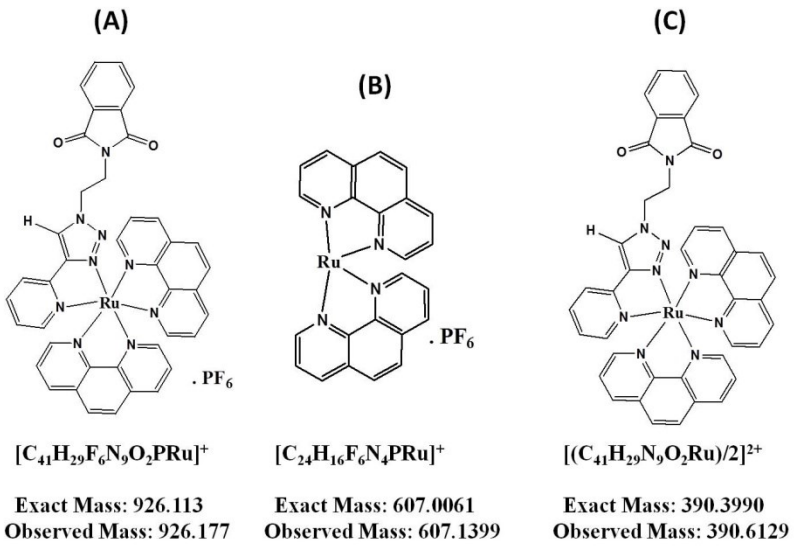

Fig.S14 HR ESI-Mass spectrum of RtpH

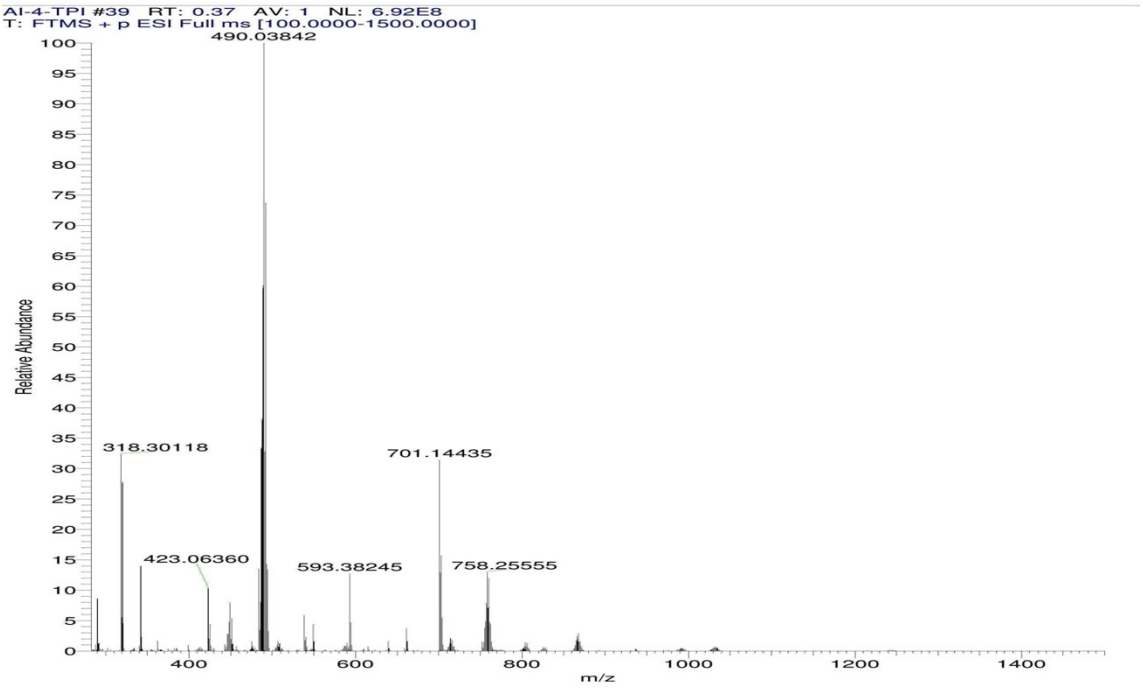

Fig. S15 HR-ESI Mass spectrum of TpI (Calculated value for $[C_{17}H_{12}IN_5O_2Ru]^+ + 2Na - H$ = 489.9747, observed = 490.0384)

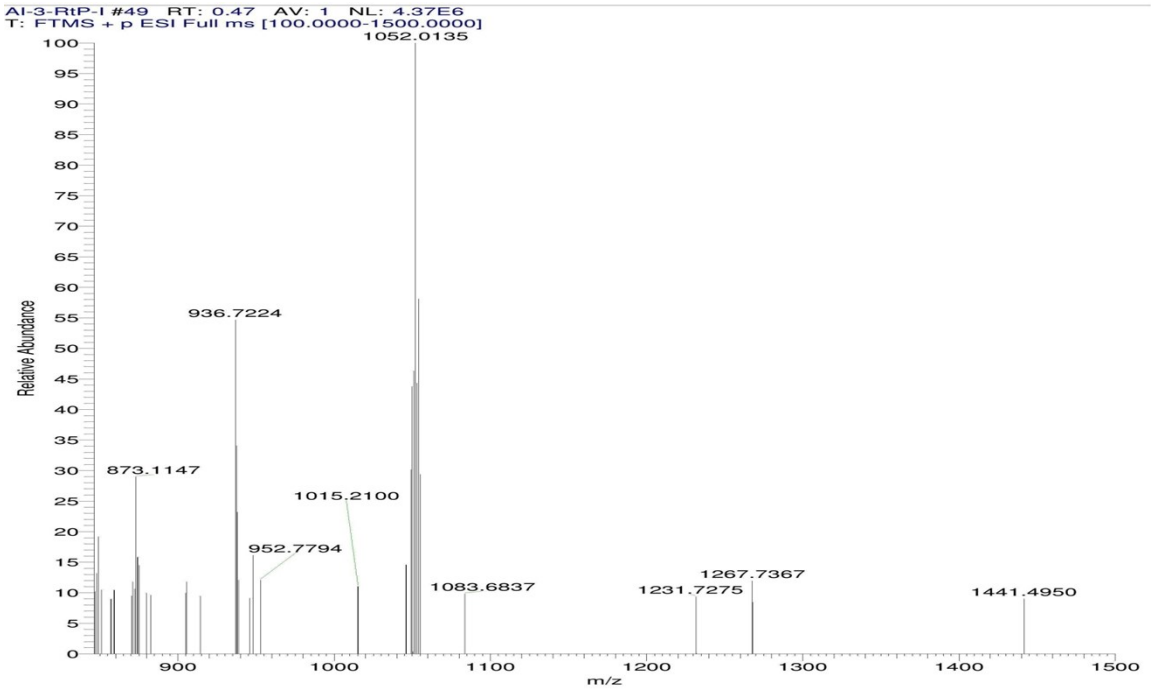

Fig. S16 HR-ESI Mass spectrum of RtpI (Calculated value for $[C_{41}H_{28}F_6IN_9O_2PRu]^+$ = 1052.0101, observed = 1052.0135)

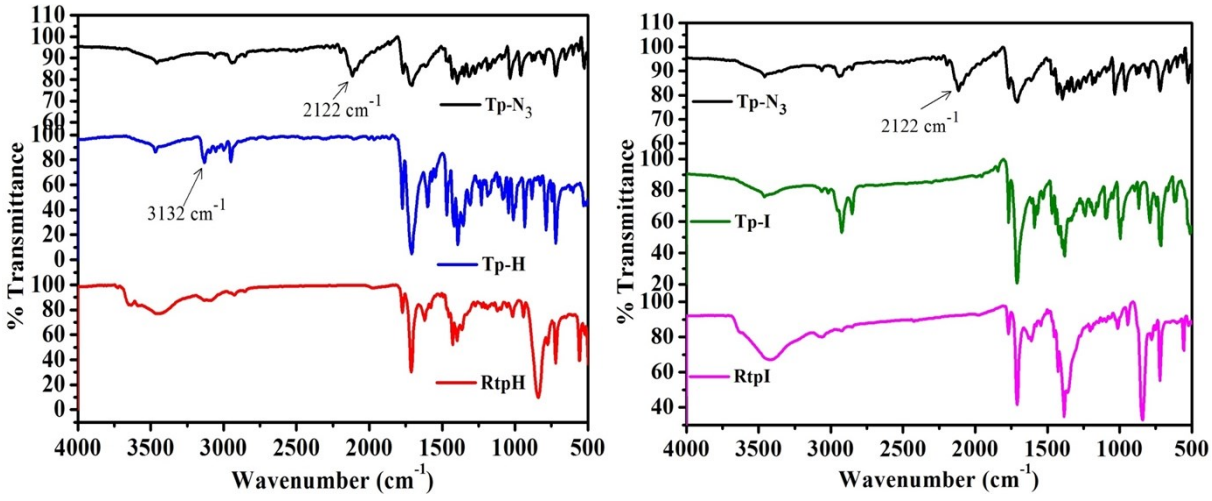

Fig.S17 FT-IR spectra of TpN_3,TpH, TpI, RtpH and RtpI.

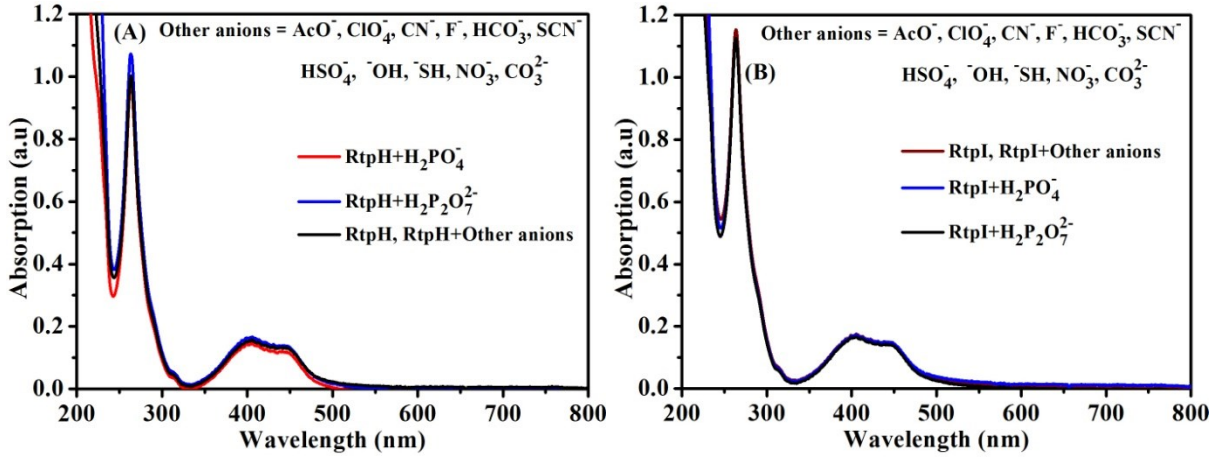

Fig.S18 (A) UV-Vis spectra of RtpH (10 μM) with various anions (5 equiv.) and phosphate anions ($H_2PO_4^-$ and $H_2P_2O_7^{2-}$) (1 equiv.), (B) Uv-Vis spectra of RtpI (10 μM) with various anions (5 equiv.) and phosphate anions ($H_2PO_4^-$ and $H_2P_2O_7^{2-}$) (1 equiv.) in CH_3CN.

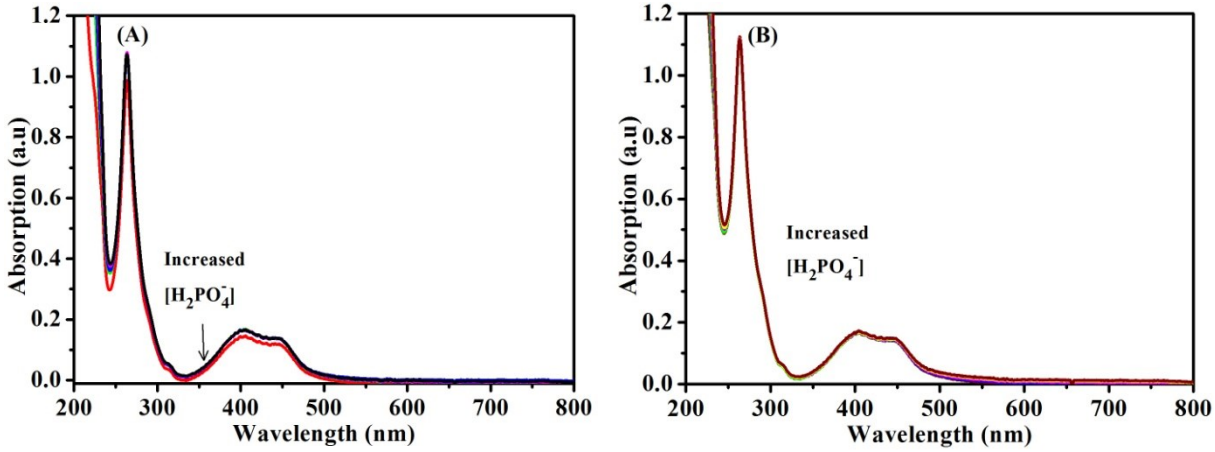

Fig.S19 (A) UV-Vis spectra of RtpH (10 μM) with the addition of $H_2PO_4^-$ anions (0-1 equiv.), (B) Uv-Vis spectra of RtpI (10 μM) with the addition of $H_2PO_4^-$ anions (0-1 equiv.) in CH_3CN.

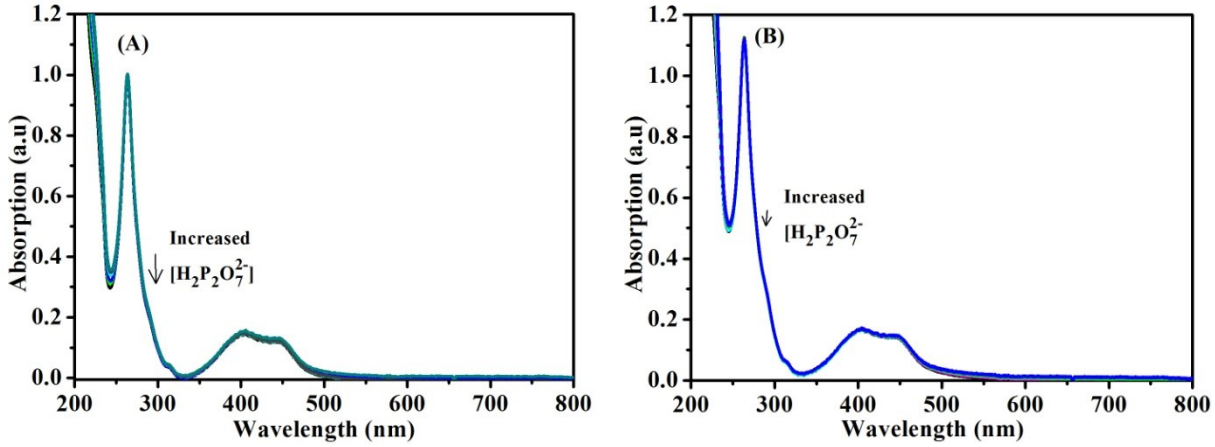

Fig.S20 (A) UV-Vis spectra of RtpI (10 μM) with the addition of $H_2P_2O_7^{2-}$anions (0-1 equiv.), (B) Uv-Vis spectra of RtpI (10 μM) with the addition of $H_2P_2O_7^{2-}$anions (0-1 equiv.) in CH_3CN.

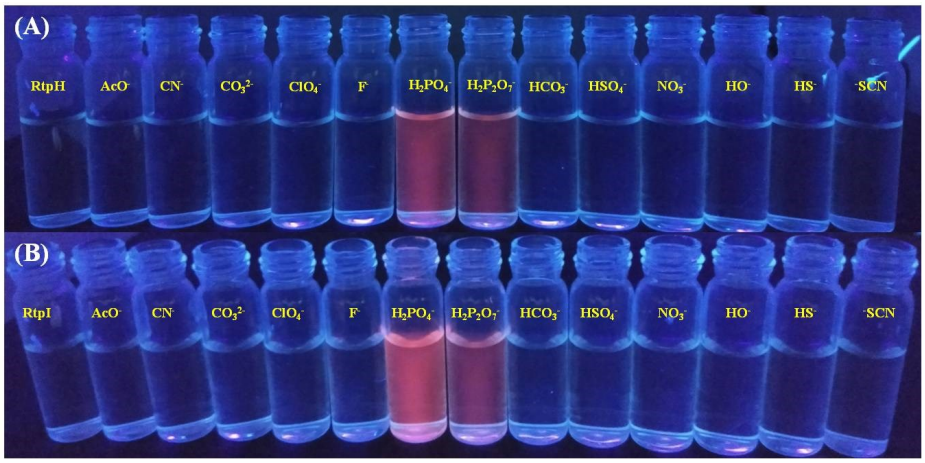

Fig.S21 Under UV light illumination, (A) RtpH and (B) RtpI with various types of anions in CH_3CN

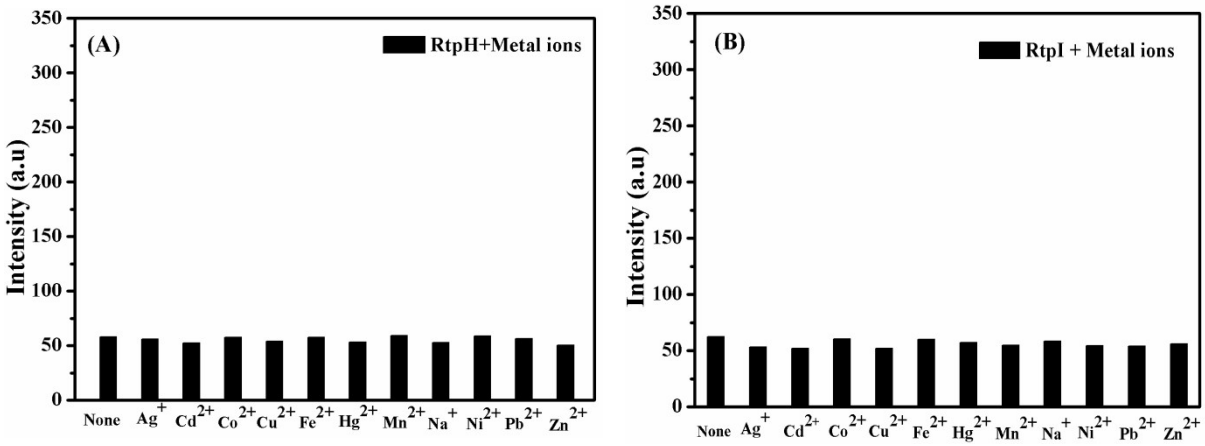

Fig.S22 (A) Emission intensity of RtpH (10 μM) with different metal ions (10 equiv.), (B) Emission intensity of RtpI (10 μM) with different metal ions (10 equiv.) in CH_3CN.

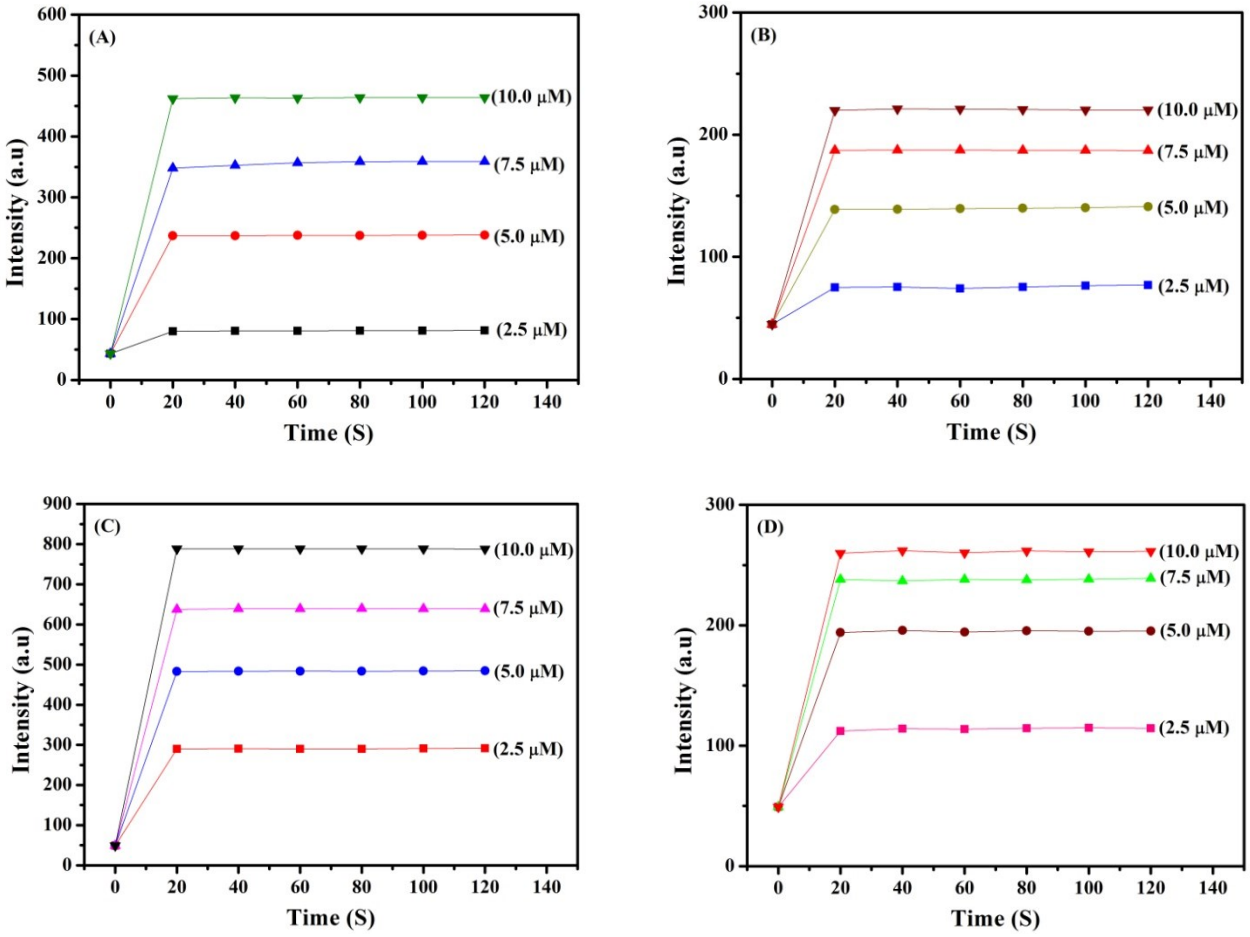

Fig.S23 (A) Time course study of RtpH (10 μM) upon addition different equivalent of $H_2PO_4^-$ (B) $H_2P_2O_7^{2-}$ in CH_3CN and time course study of RtpI (10 μM) upon addition different equivalent of $H_2PO_4^-$ (C) $H_2P_2O_7^{2-}$ (D) in CH_3CN.

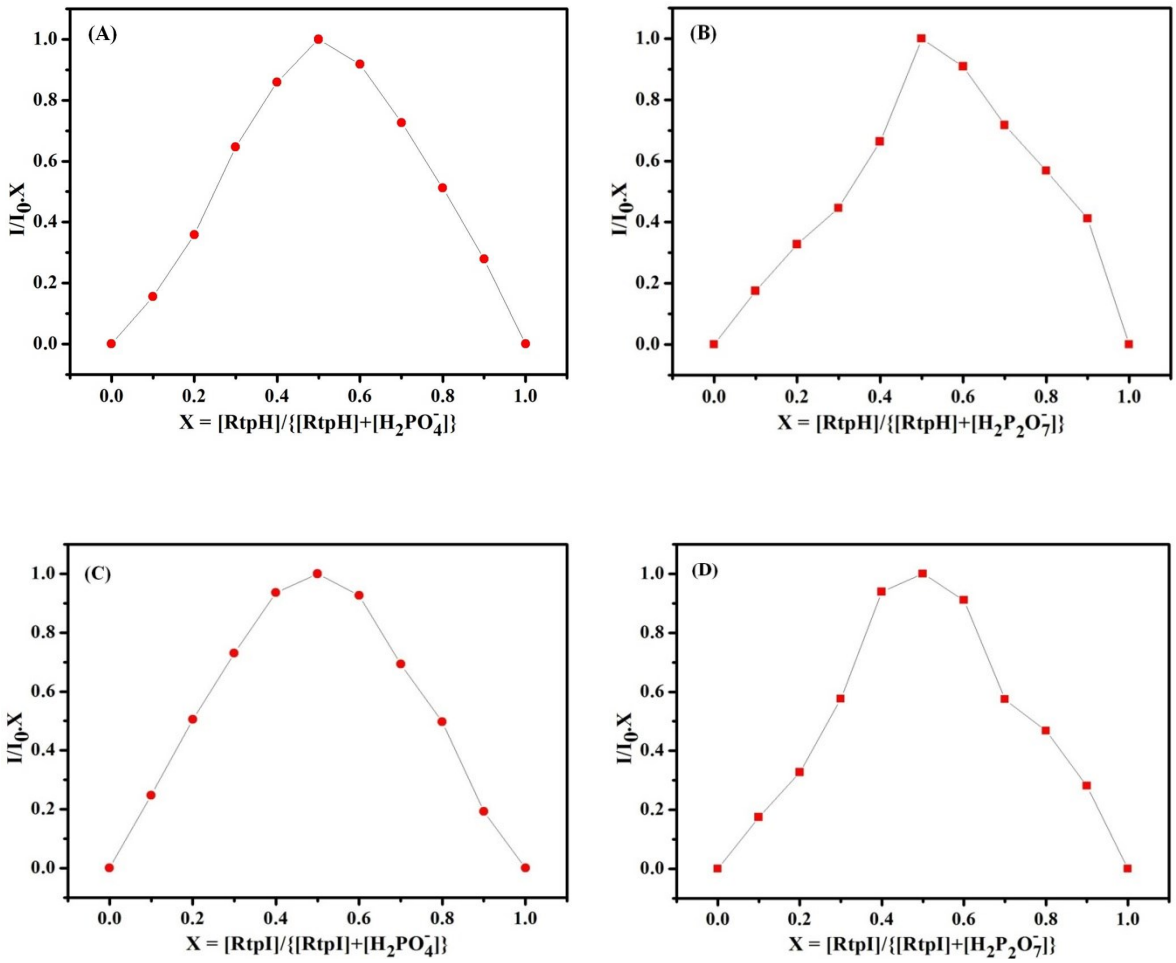

Fig.S24 Job's plot of RtpH with (A) $H_2PO_4^-$ (B) $H_2P_2O_7^{2-}$, Job's plot of RtpI with (A) $H_2PO_4^-$ (B) $H_2P_2O_7^{2-}$

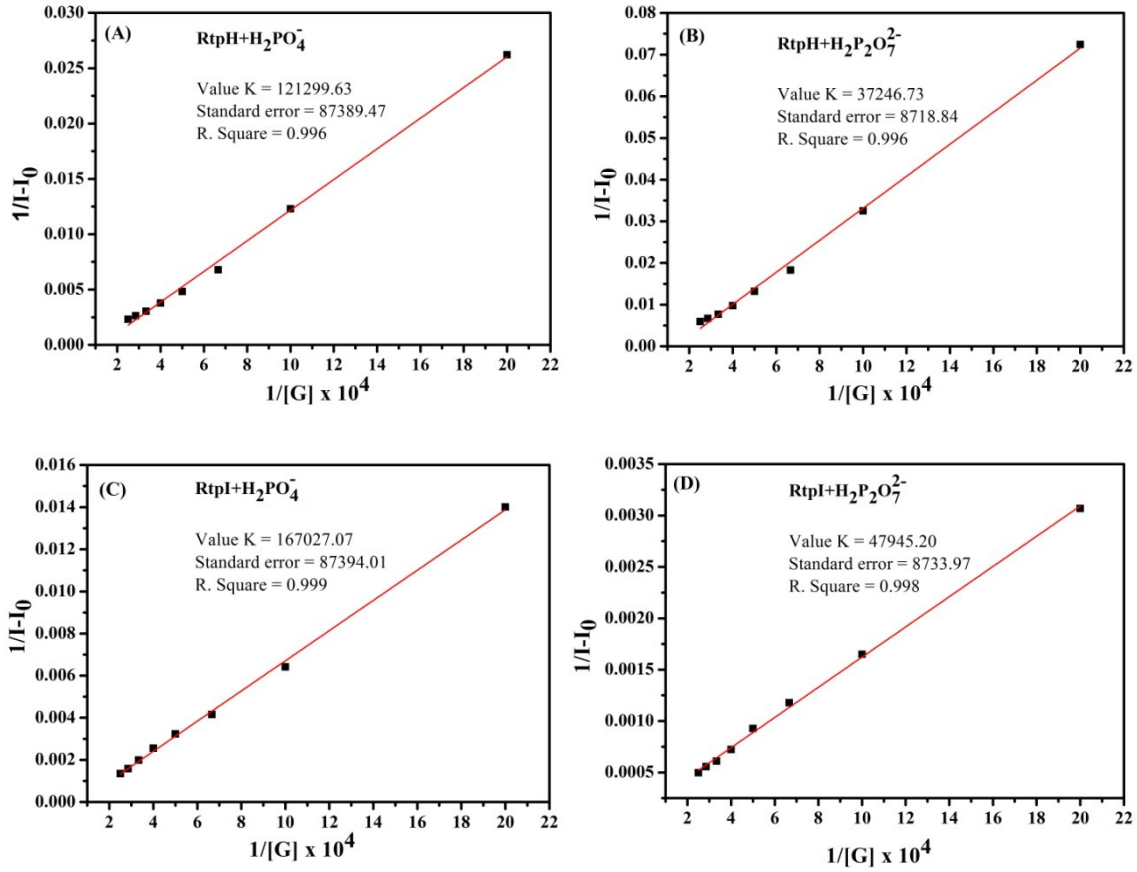

Fig. S25. Benesi-Hildebrand plot from emission titration data of RtpH (10 μM) with $H_2PO_4^-$ (A) and $H_2P_2O_7^{2-}$ (B) and of RtpI with $H_2PO_4^-$ (C) and $H_2P_2O_7^{2-}$ (D).

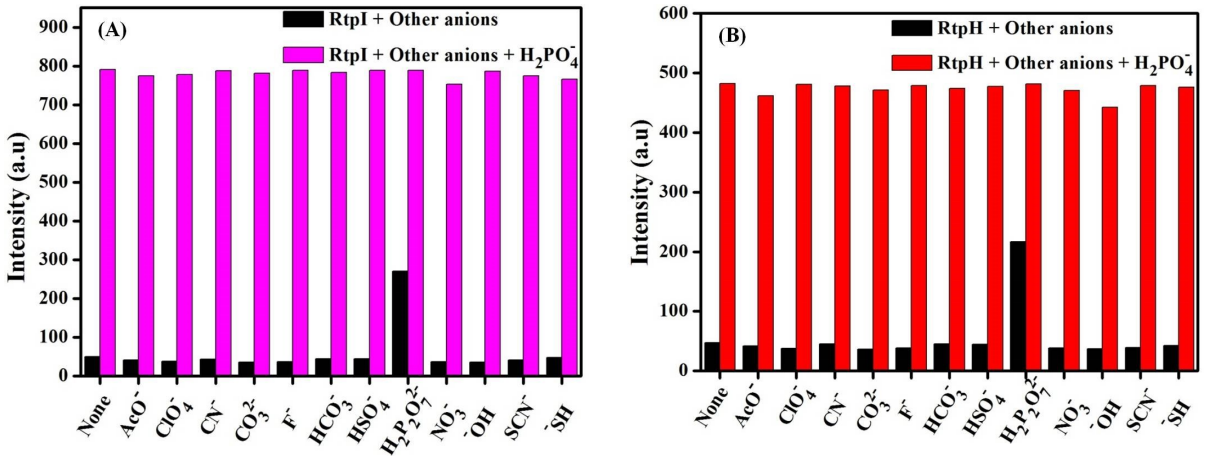

Fig.S26 (A) Interference study of RtpI (10 μM) with and without $H_2PO_4^-$ anions in presence of different anions (10 equiv.), (B) Interference study of RtpH (10 μM) with and without $H_2PO_4^-$ anions in presence of different anions (10 equiv.).

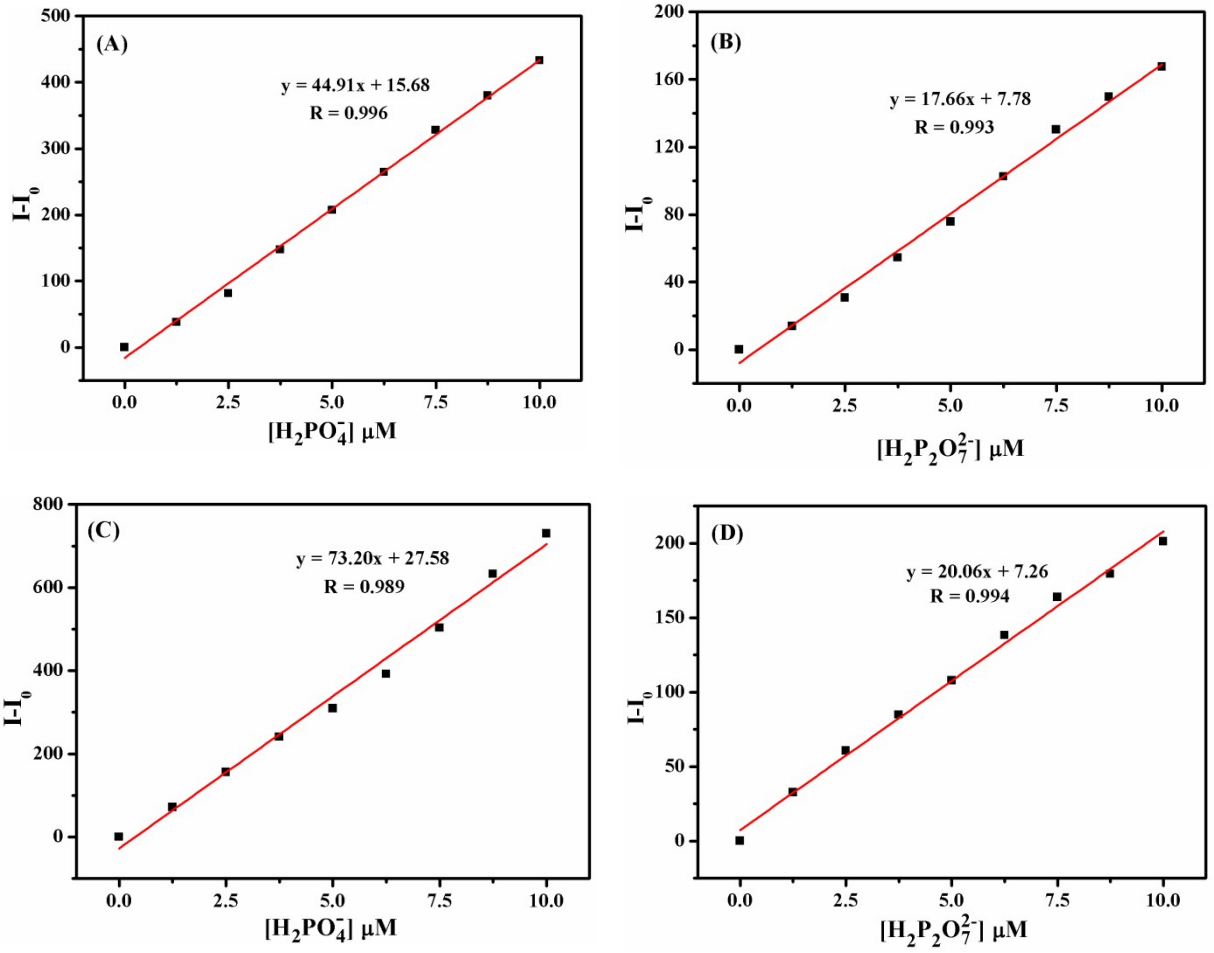

Fig.S27 A linear plot of RtpH (A, B) and RtPI (C, D) with $H_2PO_4^-$ and $H_2P_2O_7^{2-}$ in CH_3CN.

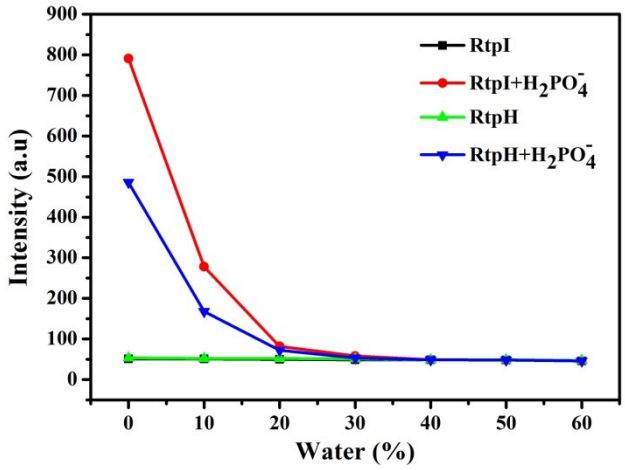

Fig. S28 The emission intensity of metalloreceptors (RtpH and RtpI, 10 µM) with phosphate anions ($H_2PO_4^-$ and $H_2P_2O_7^{2-}$, 10 µM) upon varying water percentage with CH_3CN.

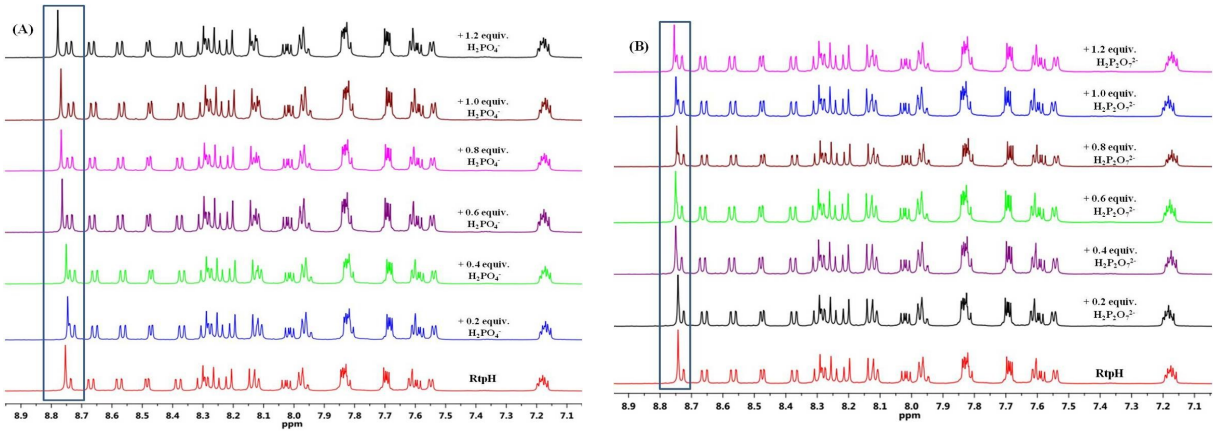

Fig.S29 (A) ^{1}H NMR titration of RtpH (7.5 mM) with $H_2PO_4^-$ (0-1.2 equiv.), (B) ^{1}H NMR titration of RtpI (7.5 mM) with $H_2PO_4^-$ (0-1.2 equiv.) in CD_3CN/D_2O (9/1, v/v).

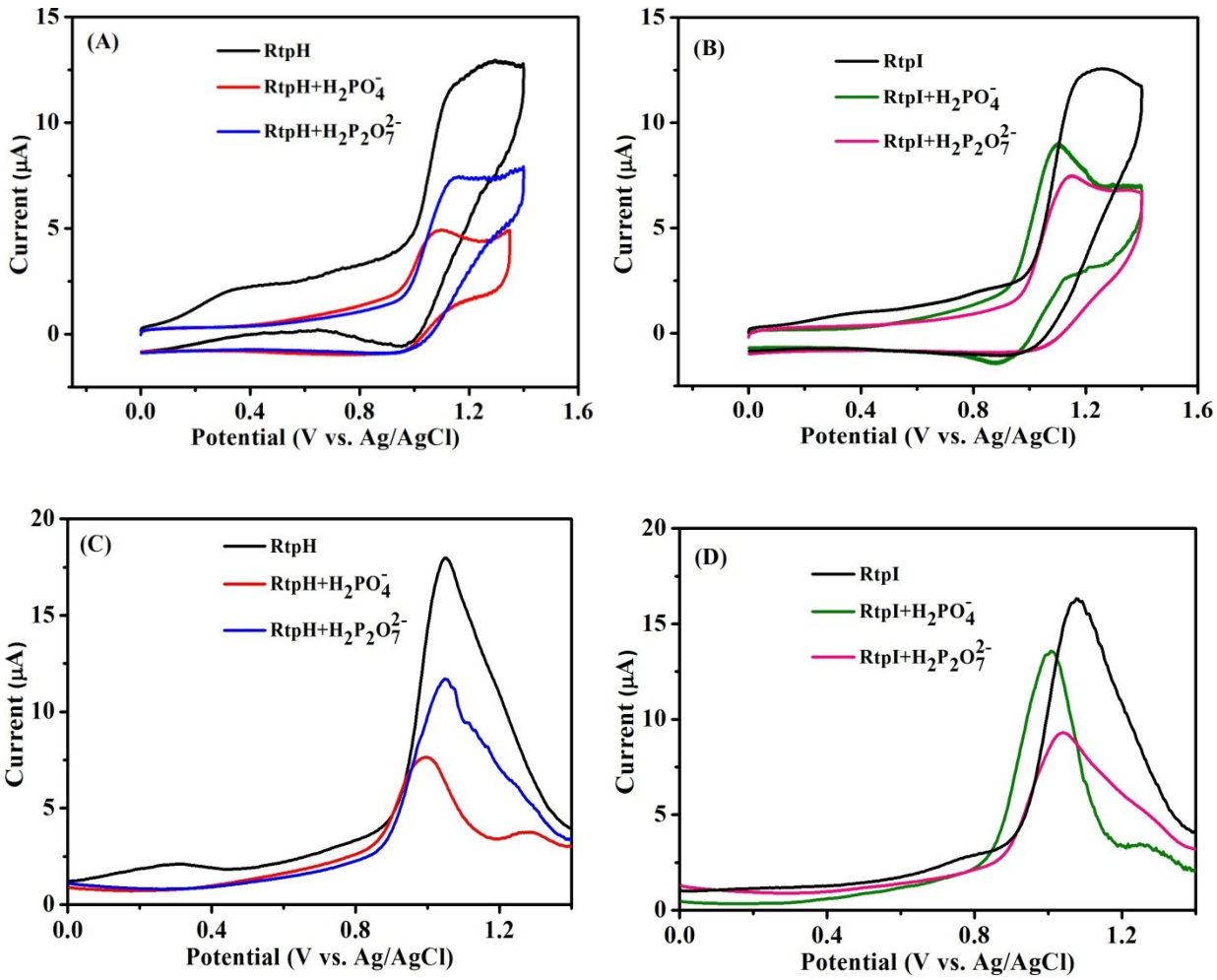

Fig.S30 (A) Cyclic Voltammetry (A and B) and Differential Pulse Voltammetry (C and D) of metalloreceptors (RtpH and RtpI) with and without phosphate anions.

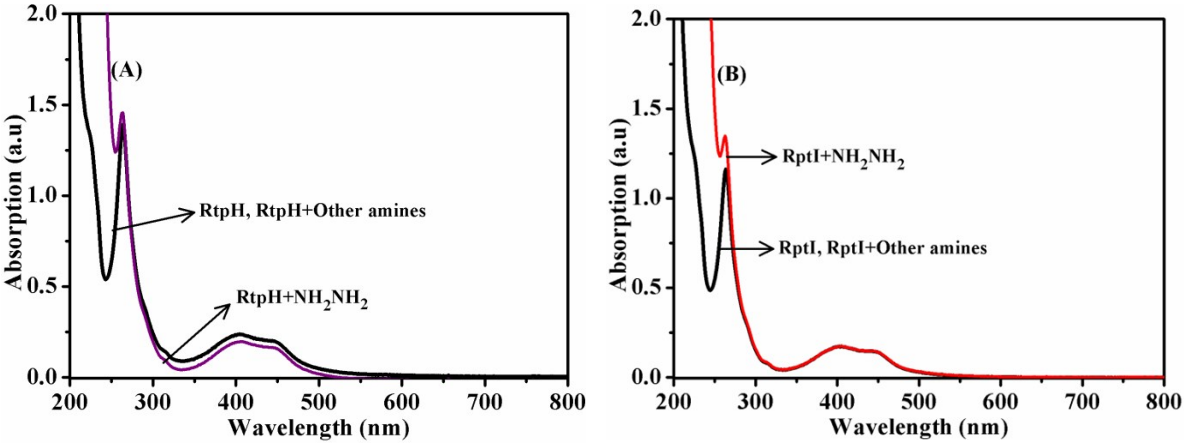

Fig.S31 (A) UV-Vis spectra of RtpH (25 μM) with various anions (10 equiv.) and hydrazine (4 equiv.), (B) UV-Vis spectra of RtpI (25 μM) with various anions (10 equiv.) and hydrazine (4 equiv.) in CH_3CN/H_2O (6/4, v/v).

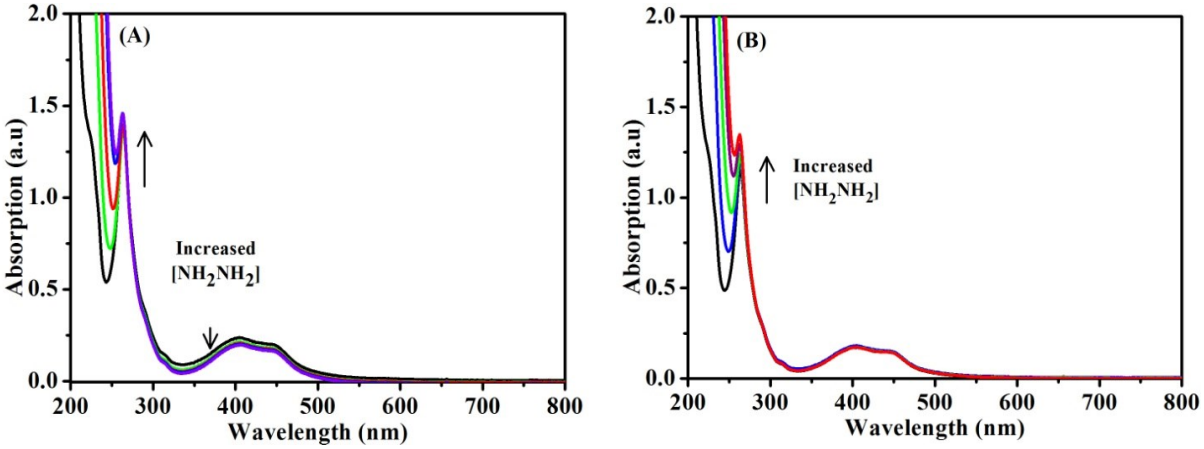

Fig.S32 (A) UV-Vis spectra of RtpH (25 μM) with the gradual addition of hydrazine (4 equiv.), (B) Uv-Vis spectra of RtpI (25 μM) with the gradual addition of hydrazine (4 equiv.) in CH_3CN/H_2O (6/4, v/v).

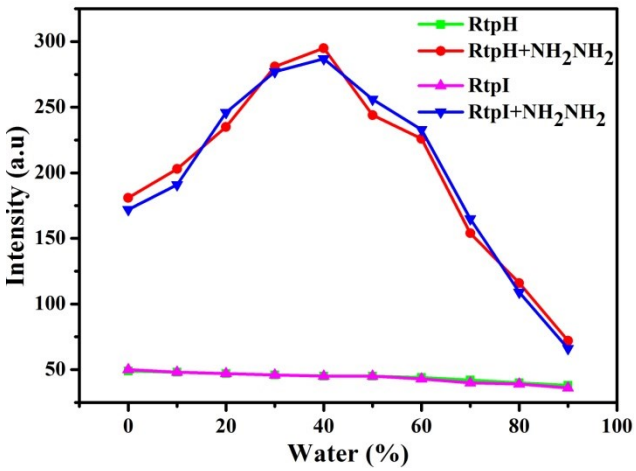

Fig. S33 The emission intensity of metalloreceptors (RtpH and RtpI, 25 μM) with hydrazine (100 μM) upon varying water percentage with CH_3CN

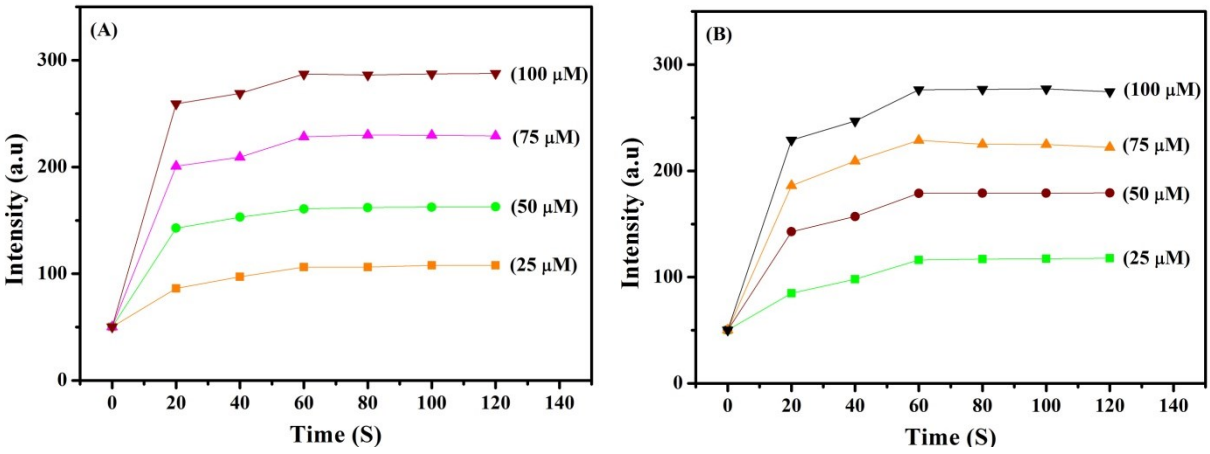

Fig. S34 (A) Time course study of RtpH (25 μM) upon addition different equivalent of hydrazine (B) Time course study of RtpH (25 μM) upon addition different equivalent of hydrazine

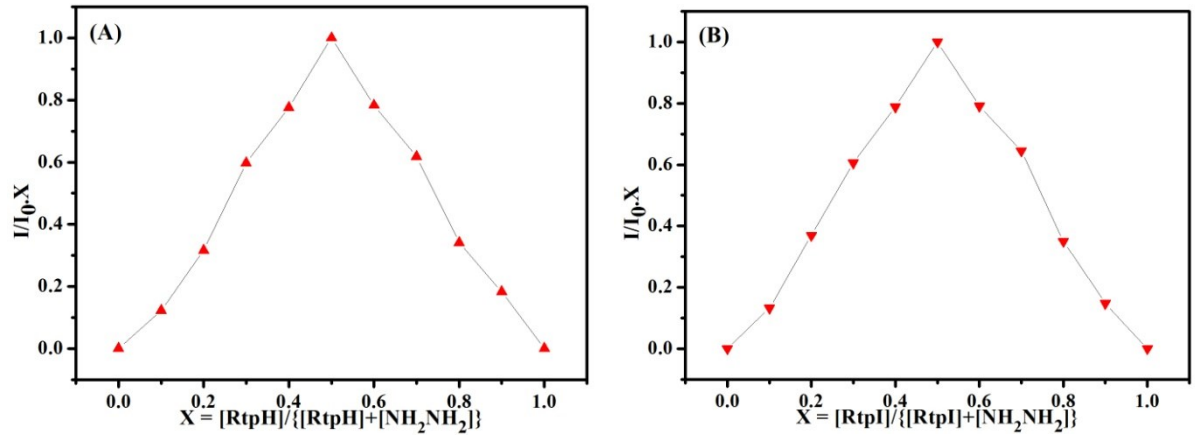

Fig.S35 (A) Job's plot of RtpH with hydrazine, (B) Job's plot of RtpI with hydrazine in CH_3CN/H_2O (6/4, v/v)

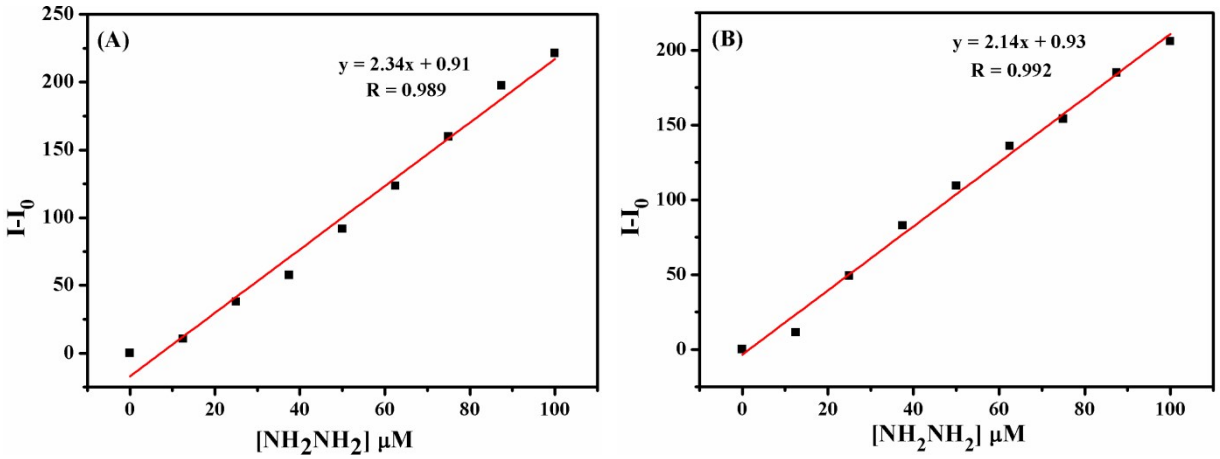

Fig.S36 (A) A linear plot of RtpH with gradual addition of hydrazine (B) A linear plot of RtpI with gradual addition of hydrazine in CH_3CN/H_2O (6/4, v/v).

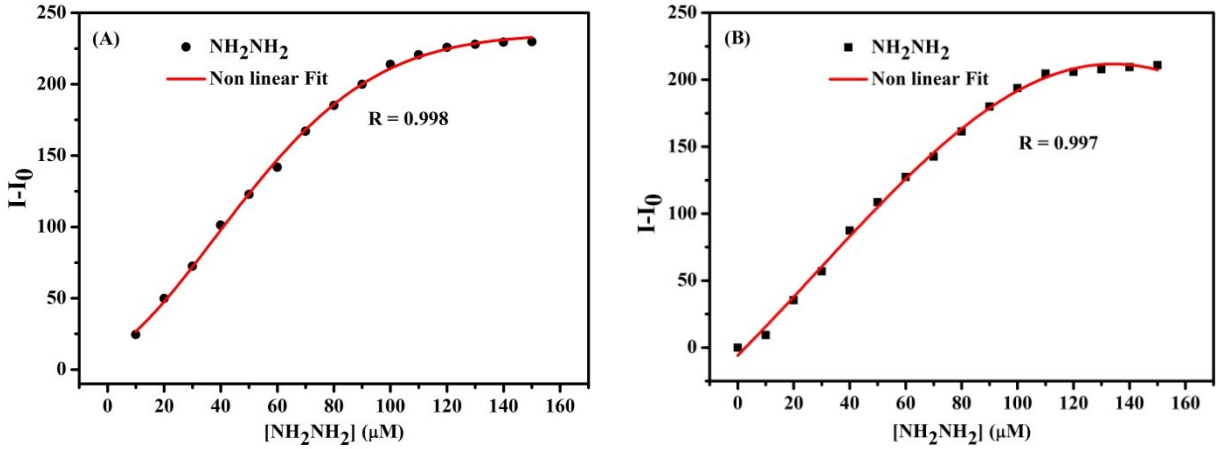

Fig. S37 (A) Non-linear fitting of RtpH (A)/ RtpI (B) (25 μM) upon addition different concentration of hydrzine

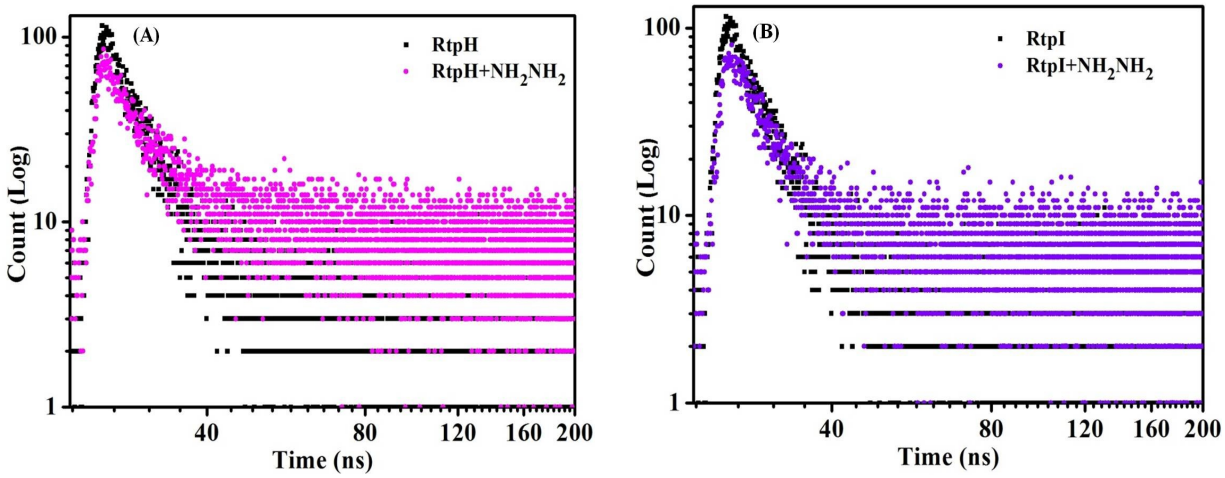

Fig.S38 (A) Lifetime decay of RtpH (10 μM) with and without hydrazine (4 equiv.), (B) Lifetime decay of RtpI (10 μM) with and without hydrazine (4 equiv.) in CH_3CN/H_2O (6/4, v/v).

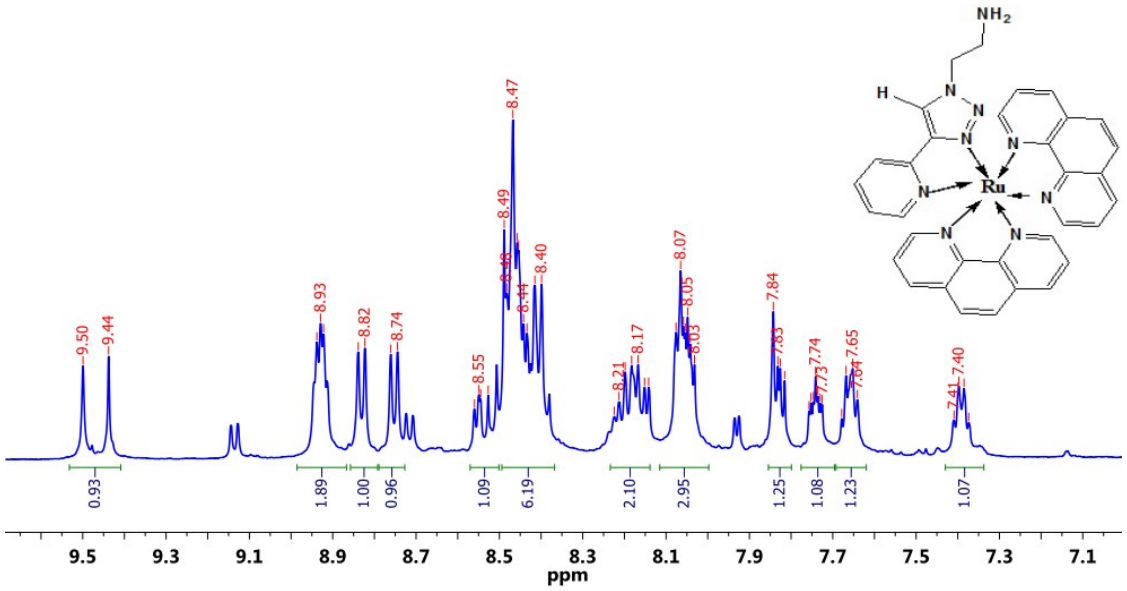

Fig. S39. Partial ^1H NMR spectrum of RtpH-NH_2 in DMSO-d_6

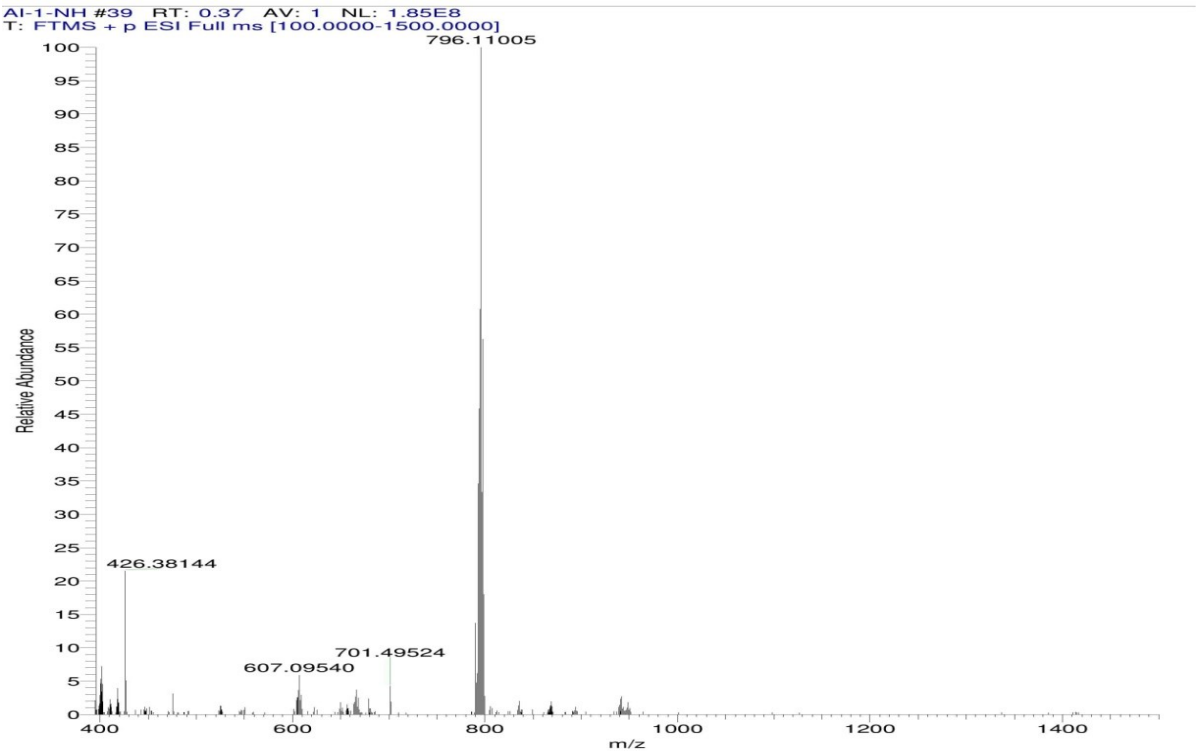

Fig. S40 HR-ESI Mass spectra of RtpH-NH_2 (Calculated value for $[C_{33}H_{26}F_6IN_9PRu]^+$ = 796.1080, observed = 796.1100)

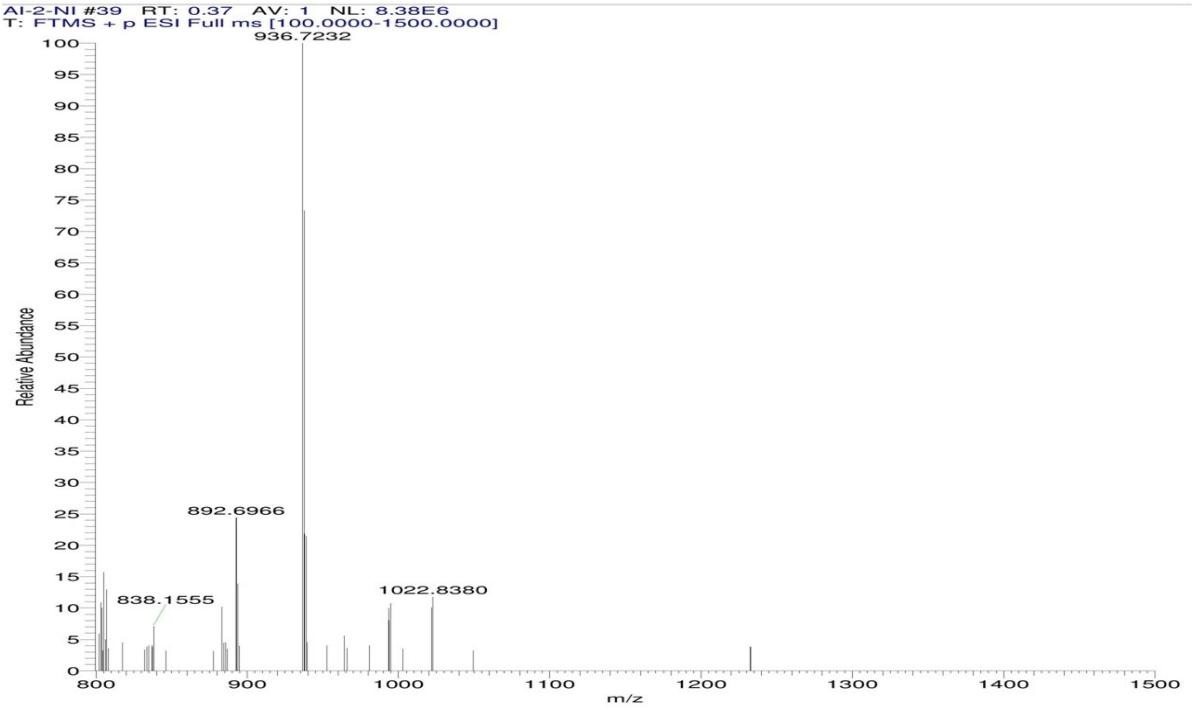

Fig. S41 HR-ESI Mass spectra of RtpI-NH_2 (Calculated value for $[C_{33}H_{27}F_6IN_9PRu]^+$ + H + 2Na = 936.7646, observed = 936.7232)

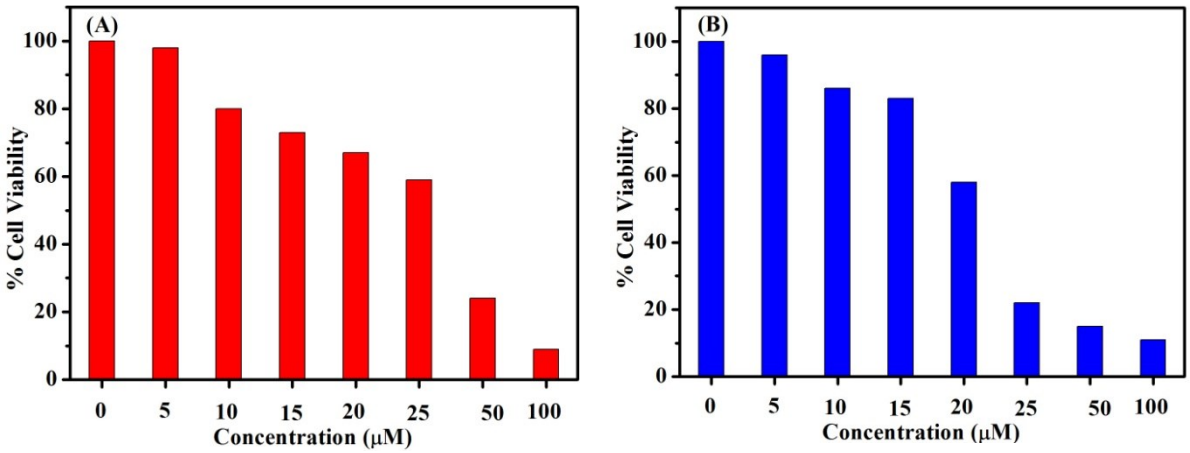

Fig.S42 Cell viability of HeLa cells in the presence of various concentrations of (A) RtpH and (B) RtpI

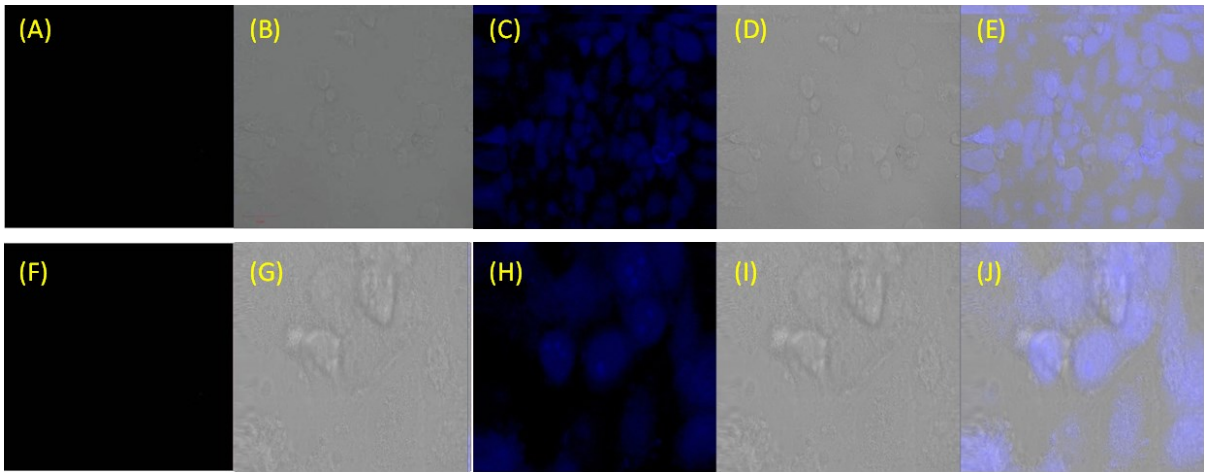

Fig. S43 Cellular uptake (HeLa) image of 25μM RtpH in dark (A), bright field (B), 4 equiv. of hydrazine treated RtpH (blue filter) (C), 4 equiv. of hydrazine treated RtpH (bright field) (D), 4 equiv. of hydrazine treated RtpH merged with RtpI (E), and 25μM RtpI in dark (F), bright field (G), 4 equiv. of hydrazine treated RtpI (blue filter) (H), 4 equiv. of hydrazine treated RtpI (bright field) (I), 4 equiv. of hydrazine treated RtpI merged with RtpH (J).

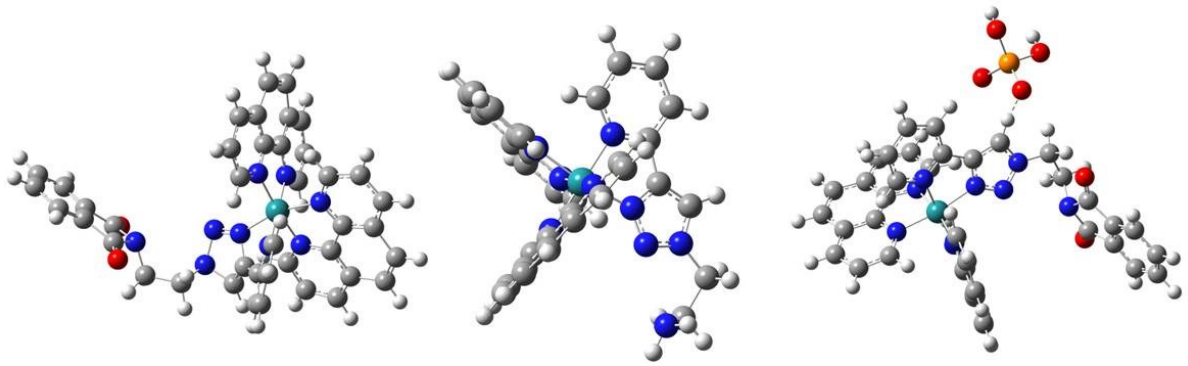

Fig.S44 Optimized structure of RtpH, RtpH-NH_2, RtpH-$H_2PO_4^-$ (from left to right)

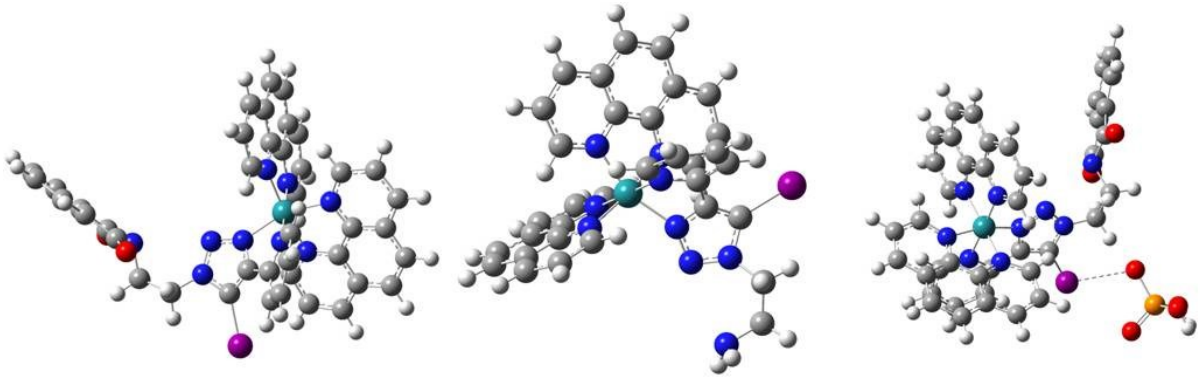

Fig.S45 Optimized structure of RtpI, RtpI-NH_2NH_2, RtpI-$H_2PO_4^-$ (from left to right)

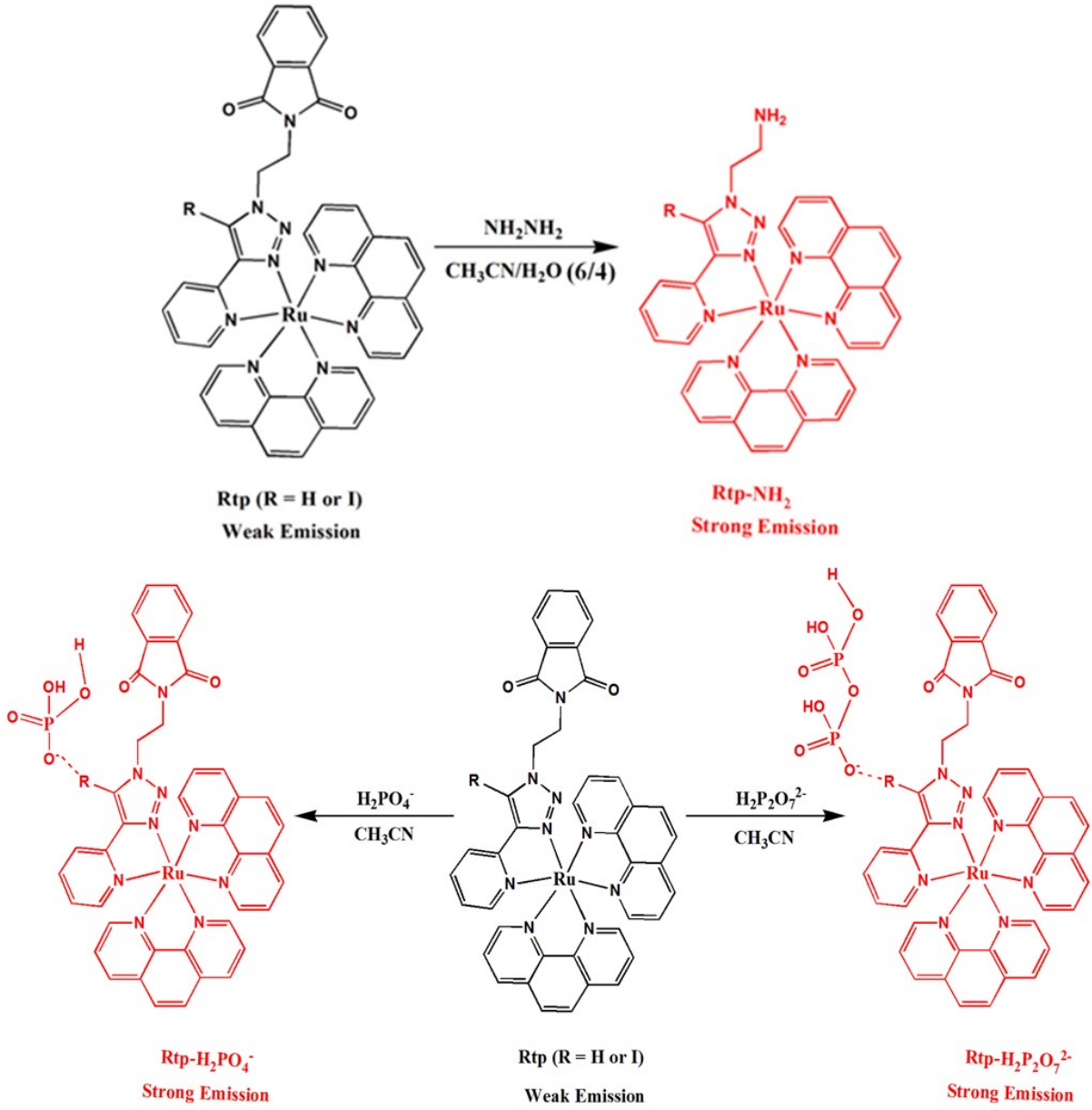

Fig.S46 Probable reaction mechanism of metalloreceptor (RtpH/RtpI) with hydrazine (above) and phosphate anions (proposed anion binding mechanism, below)

Complex	***IC_{50} Value (against HeLa cells)***
Cis-Platin	*7.2 ±1.2μM*
RtpH	*28.1 ±3.0μM*
RtpI	*22.5 ±1.7μM*

Table S1. IC_{50} Values for cis-Platin and metalloreceptors against HeLa cells